(2)

Modeling Frequency Fluctuations in Surface Contaminated Crystal Resonators

FINAL REPORT

U.S. Army Research Office
Contract/Grant No. DAAL03-87-K-0107

Yook-Kong Yong
Department of Civil & Environment Engineering
Rutgers University

July 25, 1990

UNCLASSIFIED MASTER COPY - FOR REPRODUCTION PURPOSES

SECURITY CLASSIFICATION OF THIS PAGE

REPORT DOCUMENTATION PAGE

1a. REPORT SECURITY CLASSIFICATION Unclassified	1b. RESTRICTIVE MARKINGS
2a. SECURITY CLASSIFICATION AUTHORITY	3. DISTRIBUTION/AVAILABILITY OF REPORT Approved for public release; distribution unlimited.
2b. DECLASSIFICATION/DOWNGRADING SCHEDULE	
4. PERFORMING ORGANIZATION REPORT NUMBER(S)	5. MONITORING ORGANIZATION REPORT NUMBER(S) ARO 25224.8-EL
6a. NAME OF PERFORMING ORGANIZATION Rutgers, The State University of New Jersey, College of Engineering 6b. OFFICE SYMBOL (If applicable)	7a. NAME OF MONITORING ORGANIZATION U. S. Army Research Office
6c. ADDRESS (City, State, and ZIP Code) P.O.Box 909, Piscataway, NJ 08855-0909	7b. ADDRESS (City, State, and ZIP Code) P. O. Box 12211 Research Triangle Park, NC 27709-2211
8a. NAME OF FUNDING/SPONSORING ORGANIZATION U. S. Army Research Office 8b. OFFICE SYMBOL (If applicable)	9. PROCUREMENT INSTRUMENT IDENTIFICATION NUMBER DAAL03-89-K-0107
8c. ADDRESS (City, State, and ZIP Code) P. O. Box 12211 Research Triangle Park, NC 27709-2211	10. SOURCE OF FUNDING NUMBERS PROGRAM ELEMENT NO. / PROJECT NO. / TASK NO. / WORK UNIT ACCESSION NO.
11. TITLE (Include Security Classification) Modeling of Frequency Fluctuations in Surface Contaminated Crystal Resonators (Unclassified)	
12. PERSONAL AUTHOR(S) Yook-Kong Yong	
13a. TYPE OF REPORT Final 13b. TIME COVERED FROM 7/87 TO 5/90	14. DATE OF REPORT (Year, Month, Day) 1990 July 30.
	15. PAGE COUNT 45
16. SUPPLEMENTARY NOTATION The view, opinions and/or findings contained in this report are those of the author(s) and should not be construed as an official Department of the Army position, policy, or decision, unless so designated by other documentation.	
17. COSATI CODES FIELD / GROUP / SUB GROUP	18 SUBJECT TERMS (Continue on reverse if necessary and identify by block number) Quartz thickness-shear resonators, Surface contamination, Changes in mean resonant frequency, Frequency fluctuations, Spectral density of frequency fluctuations.

19. ABSTRACT (Continue on reverse if necessary and identify by block number)

Effects of adsorption and desorption of surface contaminant molecules on mean resonant frequency and frequency fluctuations are studied. A model based on mass-loading of contaminant molecules with adsorption and desorption rates is developed. Equations relating change in mean frequency and frequency fluctuations to adsorption and desorption rates are derived. Since the adsorption and desorption rates are functions of pressure and temperature, change in mean frequency and spectral density of frequency fluctuations are studied with respect to pressure and temperature. Calculations are performed for a 10 MHz and a 525 MHz thickness-shear resonator. Frequency-temperature and frequency-pressure curves are plotted for the 10 MHz resonator. The curves do not follow a cubic polynomial function and have a magnitude in the range of 10 ppm. The mean square of frequency fluctuations under multilayer contamination is significantly greater than that under monolayer contamination. The spectral density of frequency fluctuations at 1 Hz is quite constant in a wide range of temperatures (-50 to 100°C) when the values of heat of adsorption for the second and subsequent layers is close to that for the first layer. The magnitude of spectral density of frequency fluctuations is about -120 dBc (Hz^2/Hz). The spectral density of frequency fluctuations is inversely proportional to the fourth power of the thickness if other parameters are held constant. Since the resonator frequency is inversely proportional to the thickness, the spectral density is, in effect, proportional to the fourth power of resonator frequency.

20. DISTRIBUTION/AVAILABILITY OF ABSTRACT ☐ UNCLASSIFIED/UNLIMITED ☐ SAME AS RPT. ☐ DTIC USERS	21. ABSTRACT SECURITY CLASSIFICATION Unclassified
22a. NAME OF RESPONSIBLE INDIVIDUAL	22b. TELEPHONE (Include Area Code) / 22c. OFFICE SYMBOL

DD FORM 1473, 84 MAR 83 APR edition may be used until exhausted. All other editions are obsolete.

SECURITY CLASSIFICATION OF THIS PAGE

UNCLASSIFIED

Table of Contents

	. . . . .	iii
Section 1	Statement of the Problem Studied.	1
Section 2	Theoretical Derivations and Details of Calculations.	1
Section 3	Summary of the Most Results.	2
Section 4	List of Publications.	3
Section 5	List of Participating Scientific Personnel.	4
Appendix A	Copies of Publications 1, 4 and 5.	5

THE VIEW, OPINIONS, AND/OR FINDINGS CONTAINED IN THIS REPORT ARE THOSE OF THE AUTHOR AND SHOULD NOT BE CONSTRUED AS AN OFFICIAL DEPARTMENT OF THE ARMY POSITION, POLICY, OR DECISION, UNLESS SO DESIGNATED BY OTHER DOCUMENTATION.

1. Statement of the Problem Studied.

The research was on the effects of adsorbing and desorbing molecules on the mean resonant frequency and frequency fluctuations of thickness-shear resonators, in particular, 10 MHz and 525 MHz AT-cut quartz resonators. The study examines the effects of temperature and pressure on changes in mean resonant frequency and frequency fluctuations due contaminant molecules on electrode surfaces of thickness-shear resonators. One or more species and multilayers of adsorbing molecules are treated.

The effect on resonant frequency due to an adsorbed thin mass layer, such as one or more layers of molecules, is measurable and is employed in quartz microbalances for surface adsorption studies. Physical adsorption and desorption of gas molecules from the resonator electrodes are dependent on the gas pressure, temperature, heats of adsorption and sticking coefficients. For a given resonator, the mean resonant frequency will change as a function of the number of adsorbed molecules, which in turn is a function of pressure and temperature. Since the adsorbed molecules are known to have finite lifetimes on the electrode surface, the number of adsorbed molecules at a given instant will fluctuate. Hence, short-term frequency instabilities will result if the resonator is sufficiently sensitive to fluctuations in the number of adsorbed molecules.

2. Theoretical Derivations and Details of Calculations.

The details of theoretical derivations and calculations are provided in technical publications elsewhere. The publications are listed in Section 4.

The interested reader is referred to the appendix for copies of these three papers:

1. Derivations and calculations for the effects of a monolayer or less of a single species of contaminant molecules is given in publication 1.
2. Derivations and calculations for the effects of several species of contaminant molecules in a monolayer or less of contaminant molecules is given in publication 4.
3. Derivations and calculations for the effects of several layers of a single species of contaminant molecules is given in publication 5.

3. Summary of the Most Results.

The following conclusions are applicable to frequency fluctuations and changes in mean resonant frequency induced by adsorbing and desorbing contaminant molecules in thickness-shear resonators.

1. Calculations performed for a 10 MHz thickness-shear resonator show that the mean resonant frequency can change as much as 10 ppm with temperature. In practice, this frequency change is usually masked by changes in material properties of quartz, such as elastic stiffnesses and density, which are also temperature dependent. The mean resonant frequency is also affected in the same order of magnitude by changes in the gas pressure. Frequency-temperature and frequency-pressure curves for the 10 MHz resonator cannot be described by cubic polynomial equations. (Cubic polynomial equations are used in the quartz resonator industry to describe frequency-temperature behavior.) The gas pressure would be a more suitable parameter than temperature since the quartz material properties is not significantly affected by changes in pressure.
2. Frequency fluctuations due to adsorbing and desorbing molecules are not a simple function of the percent area contaminated. A very "clean" resonator and a "dirty", namely, highly contaminated, resonator can both have low frequency fluctuations.
3. The magnitudes of frequency fluctuations due to surface contaminations is significant in VHF, UHF and thin-film thickness-shear resonators. For a 10 MHz resonator, the frequency fluctuations are generally very small (< -160 dBc Hz^2/Hz) if a monolayer or less of contaminant molecules is assumed. If the contaminant molecules are allowed to form multilayers, calculations for the 10 MHz resonator show that the magnitude of mean square frequency fluctuations at 1 Hz is in the measurable range of about -120 dBc Hz^2/Hz.
4. The spectral density of frequency fluctuations at 1 Hz for multilayer contamination is remarkably constant with changes in temperature if the heats of adsorption for the second and subsequent layers are similar to heat of adsorption of the first layer. For monolayer adsorption and desorption, the spectral density of frequency fluctuations at 1 Hz changes strongly with temperature.
5. Magnitudes of frequency fluctuations caused by surface contamination can be altered by:

   a. changing the pressure of contaminant gas

b. changing the temperature and treating the electrode surface to obtain different rates of adsorption and desorption.
c. changing the area of the electrodes. The smaller the electrode area, the higher the frequency fluctuations.

6. If all parameters except the plate thickness are held constant, the spectral density of frequency fluctuations is inversely proportional to the fourth power of plate thickness. Since the resonator frequency is inversely proportional to plate thickness, the spectral density is also proportional to the fourth power of the resonator frequency. Furthermore, if the electrode diameter decreases linearly with the operating resonator frequency, the spectral density of frequency fluctuations is approximately proportional to the sixth power of the resonator frequency.
7. Graphs of spectral density of frequency fluctuations as a function of Fourier frequency exhibit slopes ranging from $1/f^0$ to $1/f^2$. 1/f flicker noise can be obtain if the electrode surface has a wide range of values of heat of adsorption for contaminant molecules.

4. List of Publications.

1. "Resonator Surface Contamination–A Cause of Frequency Fluctuations?", Yook-Kong Yong and John R. Vig, IEEE Transactions on Ultrasonics, Ferroelectrics, and Frequency Control, Vol.36, No.4, 1989, pp 452–458.
2. "Resonator Surface Contamination–A Cause of Frequency Fluctuations?", Yook-Kong Yong and John R. Vig, Proceedings of the 42nd Annual Frequency Control Symposium 1988, pp 397–403.
3. "Modeling Frequency Fluctuations Caused by Adsorbing and Desorbing Masses in a UHF Quartz Resonator Enclosed in a Crystal Holder," Yook-Kong Yong and John R. Vig, Proceedings of the 1989 Ultrasonics Symposium, 1989, pp 455–459.
4. "Modeling Resonator Frequency Fluctuations Induced by Adsorbing and Desorbing Surface Molecules," Yook-Kong Yong and John R. Vig, IEEE Transactions on Ultrasonics, Ferroelectrics, and Frequency Control, (To be published in November, 1990).
5. "Simulation of Noise Processes in Thickness-Shear Resonators Caused by Multilayer Adsorption and Desorption of Surface Molecules," Proceedings of the 44th Annual Frequency Control Symposium, 1990, (To be published).

5. List of Participating Scientific Personnel.

1. Yook-Kong Yong, Principal Investigator, Associate Professor, Rutgers University.
2. Shunly Wang, Graduate Assistant, M.S. Civil Engineering, Rutgers University.
3. James T. Stewart, Graduate Assistant, M.S. Civil Engineering, Rutgers University.

Appendix: Copies of Publications 1, 4 and 5.

T-PAM/11/7//T-UFFC/36/4//27862

Resonator Surface Contamination—A Cause of Frequency Fluctuation?

YOOK KONG YONG
JOHN R. VIG

Reprinted from
IEEE TRANSACTIONS ON ULTRASONICS, FERROELECTRICS, AND FREQUENCY CONTROL
Vol. 36, No. 4, 1989

Resonator Surface Contamination—A Cause of Frequency Fluctuations?

YOOK KONG YONG, MEMBER, IEEE, JOHN R. VIG, SENIOR MEMBER, IEEE

Abstract—The mass loading effects of adsorbing and desorbing contaminant molecules on the magnitude and characteristics of frequency fluctuations in a thickness-shear resonator are studied. The study is motivated by the observation that the frequency of a thickness-shear resonator is determined predominantly by such mechanical parameters as the thickness of the resonator, elastic stiffnesses, mass loading of the electrodes, and energy trapping. An equation was derived relating the spectral density of frequency fluctuations to: 1) rates of adsorption and desorption of one species of contaminant molecules, 2) mass per unit area of a monolayer of molecules, 3) frequency constant, 4) thickness of resonator, and 5) number of molecular sites on one resonator surface. The induced phase noises were found to be significant in very-high-frequency resonators and are not simple functions of the percent area contaminated. The spectral density of frequency fluctuations was inversely proportional to the fourth power of the thickness if other parameters were held constant. Since the resonator frequency is inversely proportional to the thickness, the spectral density is, in effect, proportional to the fourth power of resonator frequency.

I. Introduction

SHORT-TERM FREQUENCY STABILITY (i.e., noise) is among the least well-understood resonator phenomena. Factors that have been recognized as sources of short-term instabilities include: Johnson noise, temperature fluctuations, random vibrations, acoustic losses, noise originating from interfaces between the electrodes and the quartz plate and between the mounting structure and the quartz plate, and noise due to the oscillator circuitry. Vig [1] proposed a preliminary model of frequency fluctuations induced by surface contaminations and described qualitatively the effects of such contaminations.

This paper explores and estimates the frequency fluctuations caused by adsorption and desorption of one species of molecules on the surface of a thickness-shear quartz resonator. The characteristics of such frequency fluctuations are studied. Our study is motivated by the observation that the resonant frequency of a thickness shear resonator is determined predominantly by such mechanical parameters as the thickness of the resonator, elastic stiffnesses, mass loading of the electrodes, and energy trapping. Hence, the effects on the mass loading of the stochastic characteristics of mass loading due to adsorption and desorption of contaminant molecules are considered. These effects are confined to the electrode area, since the vibrational energy is predominantly trapped within the electrodes.

Manuscript received August 1, 1988, accepted December 15, 1988. This work was supported by the U.S. Army Research Office, contract no. DAAL03-87-K-0107.

Y. K. Yong is with the Department of Civil and Environmental Engineering, Rutgers University, P.O. Box 909, Piscataway, NJ 08855-0909.

J. R. Vig is with the Frequency Control and Timing Branch, U.S. Army Electronics Technology and Devices Laboratory, SLCET-EQ, Fort Monmouth, NJ 07703-5000.

IEEE Log Number 8927882.

II. Adsorption/Desorption of Contaminant Molecules

A dynamic equilibrium exists between the resonator surface and the gas above it. This equilibrium is maintained by the rate of adsorption and desorption of contaminant molecules on the resonator surface. The area of this surface is taken as the electrode area, since most of the resonator energy is confined within the electrodes (energy trapping).

The rate of arrival of molecules at the surface can be evaluated readily from simple kinetic theory of gases. A simple form of the relationship between the rate of arrival, pressure, temperature and molecular weight of the molecule [2] is

$$r = 3.51 \times 10^{22} P/(TM)^{1/2} \text{ molecules/cm}^2\text{/s} \quad (1)$$

where P is the pressure in torrs, T the temperature is Kelvins, and M the molecular weight. In the enclosed space of a crystal resonator, the pressure will vary slightly with the fluctuations in the number of adsorbed molecules. For the present linear model, a constant pressure is assumed. If we consider the following example:

$$P = 1 \text{ torr}$$

$$T = 300°\text{K}$$

$$M = 28 \text{ (nitrogen)},$$

the rate of arrival r_0 of nitrogen molecules at a contaminant site with a spacing of 0.5 nm is $r_0 = 9.6 \times 10^5$ molecules/site/s. For a given species of molecules at a fixed temperature, the rate would be linearly dependent on the pressure. The reciprocal of this rate is the mean interarrival time τ_0.

The contaminant molecules reside on the surface for a finite time. In a simple physical adsorption process, the mean residence time [3] is

$$\tau_1 = \alpha \exp\left(E_d/(RT)\right) \quad (2)$$

where R is the gas constant $= 1.987 \times 10^{-3}$ kcal/mol K, T is temperature in Kelvins, and E_d is the desorption en-

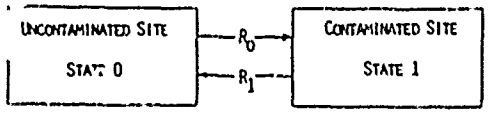

Fig. 1. Transition diagram for two states of molecular site.

ergy in kcal/mol. The exact value of the parameter α is conceptually not essential to our derivations. For subsequent calculation purposes, we assign to α a value of 1×10^{-13} seconds. If we use a typical range of values for E_d of 10 to 20 kcal/mol, the mean residence time is $\tau_1 = 2 \times 10^{-6}$ to 50 s. The mean desorption rate of molecule from the surface r_1 is the reciprocal of this mean residence time.

A monolayer, or less, of adsorbed contaminant molecules is assumed. When the system of contaminant gas and resonator surface settles down to a steady-state dynamic equilibrium, the states of the contaminant sites, which are either uncontaminated (state 0) or contaminated (state 1), can be described by steady-state probabilities. A transition diagram in Fig. 1 shows the interaction of the two states in a site. The rate in which the site enters a particular state must be equal to the rate at which it leaves. Hence, balance equations for the steady-state probabilities can be written as follows:

State	Rate Entering		Rate Leaving
0	$p_1 r_1$	=	$p_0 r_0$
1	$p_0 r_0$	=	$p_1 r_1$

(3)

where p_0 and p_1 are the steady-state probabilities of state 0 and state 1, respectively. In writing these balance equations, the assumption was made that the molecules arriving at a site would be adsorbed immediately if the site were uncontaminated but would otherwise bounce off the surface and return to the gas, that is, we assume a sticking probability of one if the site is uncontaminated and a sticking probability of zero if the site is contaminated. In reality, both probabilities generally have a value between zero and one. The exact value of the sticking probability will, depending on the desorption rate, lower or increase the magnitude of frequency fluctuations, but will otherwise not affect the logic of our derivations.

Since the site must at any given time be in either state 0 or 1, p_0 and p_1 must sum to one:

$$p_0 + p_1 = 1. \tag{4}$$

Therefore, from (3) and (4) we obtain

$$p_0 = \frac{r_1}{r_0 + r_1} \quad \text{and} \quad p_1 = \frac{r_0}{r_0 + r_1}. \tag{5}$$

The probability p_1 can be interpreted as the ratio of contaminated area to total surface area, that is, the fraction of the area contaminated. A highly contaminated, or "dirty," surface would have a value of p_1 close to unity.

III. Frequency Change Due to a Very Small Mass Loading

A. Frequency Influence Curve of an SC-Cut Strip

The effect of a very small mass on the surface of a thickness-shear resonator is investigated; namely, the effect on the resonant thickness-shear frequency. For this purpose a one-dimensional finite-element model is employed [4]. Since the ratio of the mass loading per unit area to the resonator mass per unit area is expected to be very small ($< 1 \times 10^{-4}$), the magnitude of frequency change is linearly proportional to the mass loading. Consequently, the finite element calculations for frequency change at a mass loading ratio of, say, 1×10^{-5} can be scaled linearly to yield frequency change due to mass loading of contaminant molecules.

Fig. 2 shows a unit width *SC*-cut strip subjected to a small mass loading (length 99 μm, thickness 10 nm, and density equal to that of quartz). The position of the mass is given by the coordinate along the length of the strip. The strip's resonant frequency is 3.6 MHz. If the frequency change can be plotted against the position of the mass on the strip, a curve known as the frequency influence curve is obtained. Fig. 3 gives the frequency influence curve for a mass loading (thickness 0.5 nm and length 0.5 nm) obtained from scaling the finite element calculations for the strip of Fig. 2. We observe that the mass loading has predominant frequency influence over the middle third portion of the strip. The area under this frequency influence curve represents the frequency change due to a monolayer of molecules of 0.5-nm thickness.

B. Frequency Change per Site over a 2-D Surface

For simplicity, we assume a flat frequency influence surface over the entire electrode area, although the actual frequency influence of contaminant molecules is predominantly over the middle third area of electrodes. Subsequently, it will be shown that the noise levels are inversely proportional to the surface area if other parameters are kept constant. Therefore, the assumption of a flat frequency influence surface will lower the noise levels. Based on the one-dimensional frequency influence curve of Section III-A, this assumption resulted in noise level estimates that were at least 3 dBc lower than when the actual frequency influence surface was used.

For a flat frequency influence surface, the change in frequency due to a monolayer of contaminant molecules is

$$\Delta f = f_o \frac{m'}{m} \tag{6}$$

where f_o, m', and m are, respectively, the resonator frequency, mass per unit area of a monolayer of molecules, and mass per unit area of resonator. The frequency change per site is constant

$$\xi_i = \frac{\Delta f}{N}, \quad i = 1, 2, \cdots, N \tag{7}$$

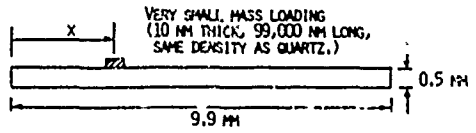

Fig. 2. *SC* cut strip (resonant frequency = 3.6 MHz) subjected to very small mass loading.

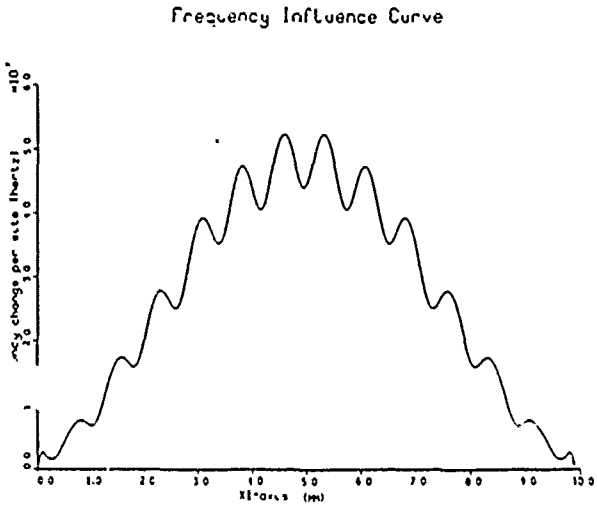

Fig. 3. Frequency influence curve of *SC*-cut strip (resonant frequency = 3.6 MHz) of Fig. 2 due to one contaminated molecular site with dimensions 0.5 × 0.5 nm, and density same as quartz.

where N is the number of sites in the active area of the resonator; that is, the area of electrode. The frequency change per site is calculated for two resonators.

Example 1: 10-MHz Thickness-Shear Resonator
Electrode area = 10 mm^2
Thickness = 0.165 mm
0.5-nm monolayer of molecules (density = quartz)
Number of sites = 4×10^{13} (0.5 nm spacing)
Δf = 30 Hz or 3 ppm
$\xi_i = 7.5 \times 10^{-13}$ Hz

Example 2: 525-MHz AT-Cut Resonator
Electrode area = 0.003 mm^2
Thickness = 3.2 μm
0.5-nm monolayer of molecules (density = quartz)
Number of sites = 12×10^9 (0.5 nm spacing)
Δf = 82 kHz or 156 ppm
$\xi_i = 6.83 \times 10^{-6}$ Hz

We observe that the frequency change per site can increase by orders of magnitude if the thickness and electrode area of resonator are reduced.

IV. Stochastic Processes

Each contaminant site yields a stochastic process that is assumed stationary, and mutually independent of other sites. The stochastic process of frequency fluctuations per site i can be written as

$$f_i(t) = \xi_i b_i(t) \qquad i = 1, 2, \cdots, N, \tag{8}$$

where $b_i(t)$ is a Bernoulli random variable with a value of one if the site is contaminated and zero otherwise. The mean or expected value of $b_i(t)$ is [5] simply

$$E[b_i(t)] = p_1, \tag{9}$$

where p_1 is the probability of the site being contaminated which, from (5), is the same as the fraction of area contaminated. The variance of $b_i(t)$ is [5]

$$\begin{aligned}\operatorname{var}[b_i(t)] &= E[b_i(t)^2] - E[b_i(t)]^2 \\ &= p_1(1 - p_1).\end{aligned} \tag{10}$$

If p_1 was substituted using (5), (10) could be expressed in terms of the adsorption and desorption rates as

$$\operatorname{var}[b_i(t)] = \frac{r_0 r_1}{(r_0 + r_1)^2}. \tag{11}$$

A. Frequency Fluctuations

The resonator frequency fluctuations induced by adsorption and desorption of contaminant molecules are obtained by summing over $2N$ sites the stochastic processes $f_i(t)$

$$f(t) = \sum_{i=1}^{2N} f_i(t) \tag{12}$$

where the factor 2 is included because the thickness shear resonator has two surfaces. The term on the right-hand side is substituted by (8) to yield

$$f(t) = \sum_{i=1}^{2N} \xi_i b_i(t). \tag{13}$$

Since $b_i(t)$ is assumed stationary, and mutually independent, the mean and variance of $f(t)$ can be derived easily by using elementary principles of statistics. The mean of $f(t)$ is, employing (9),

$$\begin{aligned}E[f(t)] &= \sum_{i=1}^{2N} \xi_i E[b_i(t)] \\ &= p_1 \sum_{i=1}^{2N} \xi_i.\end{aligned} \tag{14}$$

Equation (14) can be written in a simple form, since the sum of frequency change per site over N sites is equal to Δf

$$E[f(t)] = 2p_1 \Delta f. \tag{15}$$

Hence, the mean frequency fluctuation is twice the product of the fraction of area contaminated and frequency change due to a monolayer of molecules.

The variance of $f(t)$, σ^2, can be derived similarly, using (10),

$$\begin{aligned}\operatorname{var}[f(t)] &= \sum_{i=1}^{2N} \xi_i^2 \operatorname{var}[b_i(t)] \\ \sigma^2 &= p_1(1 - p_1) \sum_{i=1}^{2N} \xi_i^2,\end{aligned} \tag{16}$$

An expression in terms of the rates of adsorption and desorption, frequency change of a monolayer of molecules,

and total number of sites is obtained by substituting (11) and (7) into the right-hand side of (16)

$$\sigma^2 = \frac{2r_0r_1}{(r_0 + r_1)^2}(\Delta f)^2/N. \quad (17)$$

Equation (17) is valid only if a flat frequency influence surface is assumed. The variance is inversely proportional to N if other parameters were kept constant.

B. Autocorrelation and Spectral Density Functions

The autocorrelation function $R(\tau)$ is defined [6] as

$$R(\tau) = E[f(t + \tau)f(t)] \quad (18)$$

where the mean of $f(t)$ has been removed and τ is the time lag. Using (13) and assuming that the sites are mutually independent, (18) becomes

$$R(\tau) = \sum_{i=1}^{2N} \xi_i^2 E[b_i(t + \tau)\, b_i(t)]. \quad (19)$$

In the steady-state dynamic equilibrium of one species of contaminant molecule and one type of site on the resonator surface, there is one adsorption rate r_0 and one desorption rate r_1. Hence, the stochastic process has only one correlation time τ_c

$$\tau_c = (r_0 + r_1)^{-1}. \quad (20)$$

The autocorrelation function in (19) yields an exponential autocorrelation function noise [6], [7]

$$R(\tau) = \sum_{i=1}^{2N} \xi_i^2 \operatorname{Var}[b_i(t)] \exp(-|\tau|/\tau_c). \quad (21)$$

From (16) and (21), we obtain

$$R(\tau) = \sigma^2 \exp(-|\tau|/\tau_c). \quad (22)$$

The one-sided spectral density function $S_{\Delta f}(f)$ is derived by taking the Fourier transform [6] (Wiener-Khintchine relation) of (22)

$$S_{\Delta f}(f) = \frac{4\sigma^2\tau_c}{1 + (2\pi f\tau_c)^2} \quad (23)$$

where f is the Fourier frequency. On the right-hand side, σ^2 is substituted for (17) to yield the expression

$$S_{\Delta f}(f) = \frac{8r_0r_1(\Delta f)^2/N}{(r_0 + r_1)^3 + 4\pi^2f^2(r_0 + r_1)}. \quad (24)$$

It is worthwhile to describe in words the meaning of (24). The equation states that the spectral density of frequency fluctuations caused by one species of contaminant molecule and site is: 1) a function of some rational fraction of the rates of adsorption and desorption, 2) proportional to the square of the frequency change induced by a monolayer of molecules, and 3) inversely proportional to the number of sites. The spectral density function exhibits a white frequency noise process when $f \ll (r_0 + r_1)/(2\pi)$ and random walk in frequency when $f \gg (r_0 + r_1)$. There is a simple relation between the spectral densities of frequency fluctuations and phase noise of an oscillator using the resonator [8], [9]; namely,

$$S_\phi(f) = S_{\Delta f}(f)/f^2, = \frac{8r_0r_1(\Delta f)^2/N}{(r_0 + r_1)^3 + 4\pi^2f^2(r_0 + r_1)} \cdot \frac{1}{f^2}. \quad (25)$$

The spectral density of phase fluctuations is more commonly used in the field.

V. Results

The spectral densities of phase fluctuations for the two resonators in Examples 1 and 2 of Section III-B are studied over a wide range of r_0 and r_1 values. Table I shows the calculations for the phase noise of an oscillator using the two resonators at 300° K. The second column of the table was calculated using (1) and the pressure values of column 1. A molecular weight of 28 and site spacing of 0.5 nm were assumed. Column 4 was computed by employing the desorption energies in column 3 and the reciprocal of (2). Columns 5 and 6 are obtained from (5) and (20), respectively. The last two columns are the phase noises at 1 Hz, which are obtained by employing (25), parameters from Examples 1 and 2 of Section III-B, and rates from columns 2 and 4.

We observe from the second to last column of Table I that the 10 MHz thickness shear resonator yields phase noise levels which are barely measurable by today's existing noise measurement technology. The last column, on the other hand, shows that the 525-MHz resonator can produce significant levels of phase noise. We note that different noise levels are obtained for the same fraction of area contaminated.

In order to study the effects of fractional area contaminated on phase noise levels, we employ (5) to rewrite (25) in the following form

$$S_\phi(1) = \frac{8r_1p_1(1 - p_1)^2\Delta f^2/N}{r_1^2 + [2\pi(1 - p_1)]^2}, \quad 0 < p_1 < 1 \quad (26)$$

where the spectral density is evaluated at 1 Hz. If we fix the parameters Δf and N, we can plot the spectral density againt the fraction of area the contaminated for a given value of r_1, i.e., surface desorption energy. Fig. 4 shows such a plot for different values of desorption energy. The parameters for the 525 MHz resonator from Example 2 of Section III-B were used. We observe that for p_1 less than 0.1, the phase noise decreases linearly with decreasing p_1. In general, the noise level decreases rapidly when p_1 is greater than 0.9. Hence the resonator is noisiest when the fraction of the area contaminated is greater than 0.1 but less than 0.9. The magnitude of the peak noise level depends on the value of the desorption energy, the highest of which occurs in the range of E_d value from 17 to 18 kcal/mol (the parameter α of (2) being kept constant at 1×10^{-13} seconds). The value of p_1 at the peak noise level approaches unity when E_d is greater than 20 kcal/mol.

The effects of the two state variables, the pressure and temperature, on phase noise levels can be studied. Fig. 5

TABLE I
PHASE FLUCTUATIONS DUE TO SURFACE CONTAMINATIONS[a] IN 10-MHz AND 525-MHz THICKNESS-SHEAR RESONATORS

Pressure torr	r_0 1/s	E_d kcal/mol	r_1 1/s	Fraction of Area Contamination	τ_c s	10-MHz Resonator[b] 10 log $S_\phi(1)$ rad²/Hz	525-MHz Resonator[b] 10 log $S_\phi(1)$ rad²/Hz
10^3	10^9	5.49	10^9	0.500	5×10^{-10}	−196	−93
10^0	10^6	9.61	10^6	0.500	5×10^{-7}	−166	−63
10^{-3}	10^3	13.7	10^3	0.500	5×10^{-4}	−136	−33
10^{-5}	10	16.5	10	0.500	5×10^{-2}	−117	−13
10^{-6}	1	17.8	1	0.500	0.5	−117	−13
10^{-7}	10^{-1}	19.2	10^{-1}	0.500	5	−126	−22
10^{-9}	10^{-3}	22.0	10^{-3}	0.500	500	−147	−42

[a]A heavier contaminant molecule will raise the phase-noise levels.
[b]Resonators from Examples 1 and 2 of Section III-B.

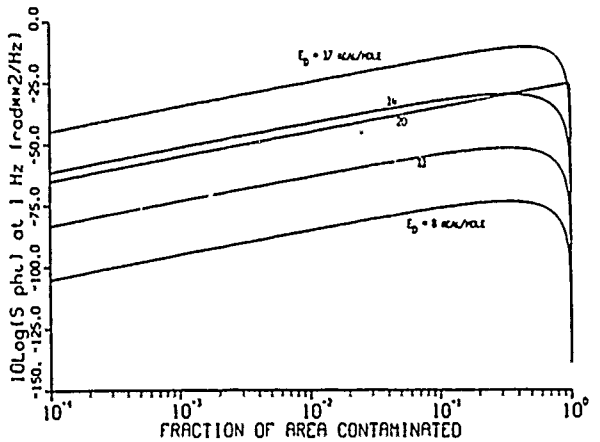

Fig. 4. Effects of fraction of area contaminated on spectral density of phase fluctuations at 1 Hz (525-MHz resonator).

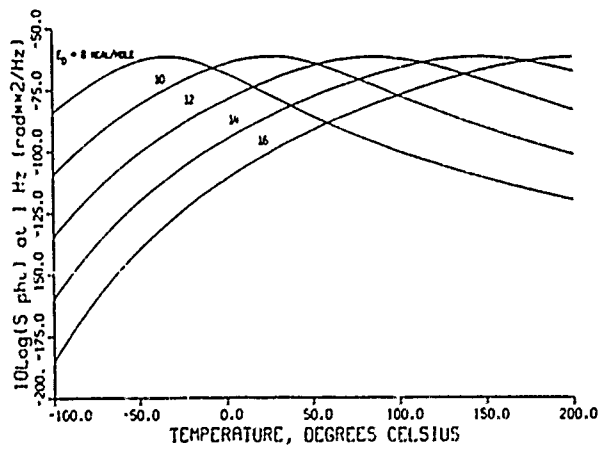

Fig. 5. Phase noise-temperature curves for 525-MHz resonator.

exhibits the phase noise-temperature curves of the 525-MHz resonator at a pressure of 0.1 torr. We observe that when the temperature is increased from a reference temperature of, say, 25°C, the phase noise levels can increase or decrease depending on the values of E_d. The turnover temperatures of the curves increase with increasing values of E_d.

Fig. 6 shows the phase noise-pressure curves of the 525-MHz resonator at a temperature of 300° K. The overall shapes of the curves look similar to the curves in Fig. 5 but the turnover pressures decrease with increasing values of E_d. We observe that a decrease in pressure does not necessarily imply a decrease in noise levels.

Fig. 7 shows the spectral density of phase fluctuations for the 525-MHz resonator using (25) and r_0 and r_1 equal to 100 and 0.1 s^{-1}. For Fourier frequencies of less than 10 Hz, the white frequency fluctuations predominate. The random walk frequency noise is dominant at Fourier frequencies greater than 50 Hz.

We can make another important observation based on the parameters in (24) or (25). For this purpose, we replace the term Δf in (24) using (6)

$$S_{\Delta f}(f) = \frac{8r_0r_1(f_om'/m)^2/N}{(r_0 + r_1)^3 + 4\pi^2f^2(r_0 + r_1)}. \quad (27)$$

Upon a first glance, it would appear that the spectral density is proportional to the square of the resonator frequency f_o, if other parameters were held constant. But the frequency of a thickness-shear resonator is inversely proportional to the thickness of the plate

$$f_o = k/h \quad (28)$$

where h is the resonator thickness and k is the frequency constant determined by the elastic constants and overtone of thickness shear vibration. The mass per unit area is also related to the thickness

$$m = \rho h \quad (29)$$

where ρ is the resonator density. Substituting (28) and (29) into (27), we obtain

$$S_{\Delta f}(f) = \frac{8r_0r_1(km')^2/(Nh^4)}{(r_0 + r_1)^3 + 4\pi^2f^2(r_0 + r_1)}. \quad (30)$$

Hence, the spectral density is inversely proportional to the fourth power of h. Since the resonator frequency is inversely proportional to h, (30) shows, in effect, that the

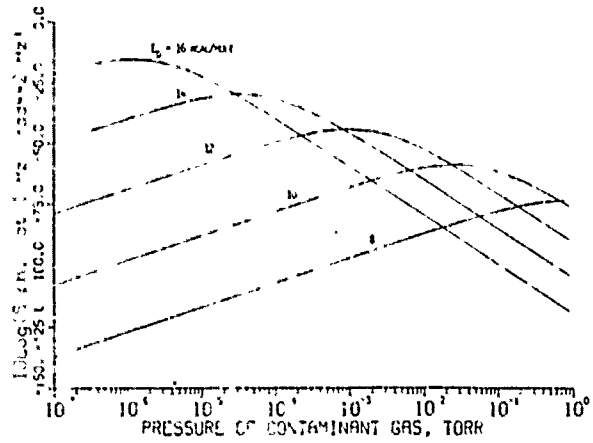

Fig. 6. Phase noise-pressure curves for 525-MHz resonator.

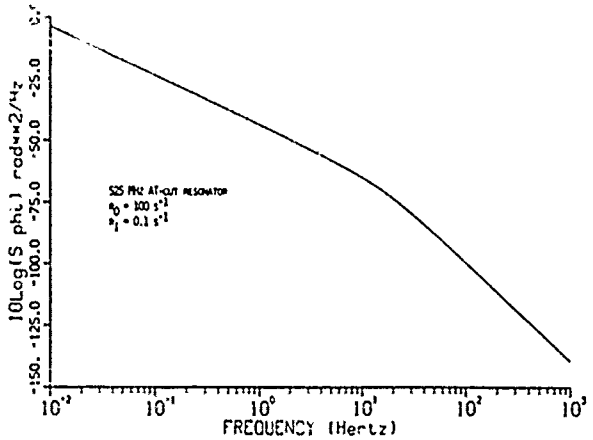

Fig. 7. Spectral density of phase fluctuations for 525-MHz resonator.

spectral density is proportional to the fourth power of resonator frequency. Experimental results relating the flicker frequency fluctuations to the fourth power of quartz resonator frequency were reported by Parker [9] and Kroupa [10].

In an actual thickness shear resonator, the electrode area usually decreases with increasing resonator frequency, which leads to decreasing values of N and increasing magnitudes of phase noise. If the electrode diameter decreases with frequency by a linear factor, the number of sites N will decrease by the square of this linear factor, and the spectral density of frequency fluctuations, according to (30) will be proportional to the sixth power of the resonator frequency. This tends to agree with the phenomenological law proposed by Gagnepain, Uebersfeld, Goujon, and Handel [11]; namely, that the spectral density of frequency fluctuations is proportional to the reciprocal of the fourth power of resonator unloaded Q-factor

$$S_{\Delta f}(f) \alpha \frac{f_o^2}{Q_u^4}.$$

If the product $Q_u f_o$ is constant, as is usually the case, then their spectral density is proportional to the sixth power of resonator frequency

$$S_{\Delta f}(f) \alpha f_o^6.$$

In a recent review paper, Weissman [12] reported that a superposition of a number of Lorentzian spectra similar to (30) will yield flicker frequency fluctuations. When more than one species of contaminant molecules and sites are present in the contaminant gas-resonator surface system, the stochastic process has more than one correlation time. Hence, depending on the distribution of the correlation times, the basic model in (30) can produce flicker frequency fluctuations over some range of Fourier frequencies. Most observed noise at 1 Hz is flicker frequency rather than white or random walk.

VI. Conclusion

The following conclusions are applicable to phase noise in thickness shear resonators induced by one species of contaminant molecule and site.

1) The phase noise is not a simple function of the percent area contaminated, as shown in (26). A very "clean" resonator, and a "dirty," that is, highly contaminated, resonator can both have low noise levels.
2) The phase noise due to surface contaminations can be significant in VHF, UHF, and membrane resonators. For the 10-MHz resonator only the worst case calculations begin to approach the observed noise levels. In contrast, for the 525-MHz resonator, the worst case calculations are too high for observed noise levels.
3) Surface-contamination-caused noise levels can be altered by:
   a) changing the pressure of the contaminant gas above the surface,
   b) changing the temperature and treating the surface to obtain different rates of adsorption and desorption,
   c) changing the area of the electrode. The smaller the area, the higher the noise levels.
4) If all parameters except the thickness h are held constant in (30), the spectral density of frequency fluctuations is inversely proportional to the fourth power of h. Since the resonator frequency is inversely proportional to h, the spectral density is also proportional to the fourth power of the resonator frequency. Furthermore, if the electrode diameter decreases linearly with the operating resonator frequency, the spectral density of frequency fluctuations is approximately proportional to the sixth power of the resonator frequency.

One possible experiment to verify the findings in this paper may involve measuring the phase noise of a ultra-high-frequency resonator while it is in a controlled atmosphere in a vacuum chamber, and then decreasing the pressure gradually. Extra care must be taken to keep constant all other parameters in (30) and to reduce other noise sources, such as random vibrations, temperature fluctuations, noise due to oscillator circuitry, etc., so as not to interfere with the measurements. The gas above the resonator must con-

sist of essentially one species of contaminant molecules. A concomitant experiment would entail keeping the pressure constant and varying the temperature instead. The effects of decreasing thickness on phase noise levels in a given high-frequency resonator should also be studied.

Acknowledgment

The authors thank Charles A. Greenhall at Jet Propulsion Laboratory, and Thomas E. Parker at Raytheon Company, for their helpful comments. The authors also thank James T. Stewart at Rutgers University, for computing the one-dimensional frequency influence curve. The reviewers' comments were helpful and appreciated.

References

[1] J. R. Vig, "The effects of surface contamination on the noise and drive-level sensitivity of piezoelectric resonators," Research and Development Tech. Rep. SLCET-TR-87-5, ADA181299, May 1987.
[2] M. Prutton, *Surface Physics*, 2nd ed. Oxford: Clarendon Press, 1983, pp. 5-6.
[3] ——, *Surface Physics*, 2nd ed. Oxford: Clarendon Press, 1983, pp. 103-104 and pp. 110-112.
[4] Y. K. Yong, "On the use of 1-D finite elements for the temperature behavior of a contoured and partially plated SC-cut resonator," in *Proc. IEEE 1987 Ultrason. Symp.*, 1987, pp. 353-358.
[5] S. M. Ross, *Introduction to Probability Models*, 3rd ed. Orlando, FL: Academic Press, 1985, ch. 2, pp. 21-82.
[6] J. S. Bendat and A. G. Piersol, *Random Data, Analysis and Measurement Procedures*, 2nd ed. New York: Wiley-Interscience, 1986, ch. 5, pp. 109-163.
[7] R. F. Voss, "$1/f$ (flicker) noise: A brief review," in *Proc. 33rd Annu. Symp. Freq. Contr.*, 1979, pp. 40-46.
[8] D. A. Howe, D. W. Allan, and J. A. Barnes, "Properties of signal sources and measurement methods," in *Proc. 35th Annu. Symp. Freq. Contr.*, 1981, pp. A1-A47.
[9] T. E. Parker, "$1/f$ frequency fluctuations in quartz acoustic resonators," *Appl. Phys. Lett.*, vol. 46, no. 3, pp. 246-248, 1985.
[10] V. F. Kroupa, "The state of the art of the flicker frequency noise in BAW and SAW quartz resonators," *IEEE Trans. Ultrason., Ferroelect. Freq. Contr.*, vol. 35, no. 3, pp. 406-420, May 1988.
[11] J. J. Gagnepain, J. Uebersfeld, G. Goujon, and P. Handel, "Relation between $1/f$ noise and Q-factor in quartz resonators at room and low temperatures, first theoretical interpretation," in *Proc. 35th Annu. Freq. Contr. Symp.*, 1981, pp. 476-483.
[12] M. B. Weissman, "$1/f$ noise and other slow, nonexponential kinetics in condensed matter," *Rev. Mod. Phys.*, vol. 60, no. 2, Apr. 1988, pp. 537-571.

Yook Kong Yong (M'86) received the B.S. degree in civil engineering from Lafayette College, Easton, PA, in 1979, the M.A. and Ph.D. degrees in structures/mechanics from Princeton University, Princeton, NJ, in 1981 and 1984, respectively.

He is an Associate Professor with the Department of Civil/Environmental Engineering, Rutgers University, New Brunswick, NJ. His research interests are in the noise characteristics, frequency-temperature behavior, and numerical modeling of crystal resonators, material behavior of high-strength concrete in structural components and nonlinear numerical modeling of concrete. The results of his research have been presented at symposia and have been published in about 20 professional papers.

Dr. Yong is a member of the IEEE UFFC Society, Acoustical Society of America, AAAS, American Society of Civil Engineers and American Concrete Institute. He is also a member of the ACI Committee E801 on student concrete projects, and the Technical Program Committee of the 1989 IEEE Ultrasonics Symposium. He belongs to the Chi Epsilon Civil Engineering Honor Society, and Tau Beta Pi Engineering Honor Society. He is the recipient of the Carrol Phillips Bassett Civil Engineering Prize from Lafayette College.

John R. Vig (M'72-SM'84) was born in Hungary in 1942. He received the B.S. degree in physics from the City College of New York in 1964, and the M.S. and Ph.D. degrees from Rutgers University, New Brunswick, NJ, in 1966 and 1969, respectively.

From 1969 to 1972 he served as an Officer in the U.S. Army, stationed at the R&D laboratories of the Army Electronic Command, Fort Monmouth, NJ, where he developed a superconductive tunable filter. Since 1972 he has been employed as a civilian research scientist at Fort Monmouth, working primarily on the experimental aspects of quartz crystal devices. Specific areas of interest have included the properties of quartz, resonator fabrication technology (cleaning, etching, polishing, X-ray orienting, packaging, etc), the effects of design and processing parameters on stability, and the developments of SC-cut crystals for high-stability applications. He is currently Chief of the Frequency Control and Timing Branch in the U.S. Army Electronics Technology and Devices Laboratory, Fort Monmouth. He leads a multidisciplinary research program aimed at the development of high-stability frequency control devices and clocks for future Army communication, navigation, identification, and radar systems.

Dr. Vig served as the General Chairman of the UFFC Society's Annual Frequency Control Symposium from 1982 to 1988. Since 1972 he has been a member of the Technical Program Committee of the Frequency Control Symposium. He served from 1982 to 1986 as a member of the Technical Program Committee of the Quartz Devices Conference, and since 1982, on the Executive Committee of the Precise Time and Time Interval Applications and Planning Meeting. He has been the Principle United States Member of the NATO Working Group on Frequency Control Devices since 1981 He was appointed to the IEEE Committee on Time and Frequency (TC-3) in 1979, and in 1985 as the IEEE Representative on the Hoover Medal Board of Award. He has received the highest R&D award bestowed by the U.S. Army, the Army Research and Development Achievement Award, in 1979, 1983, and 1987. The results of his research have been presented at symposia and have been published in more than 50 professional papers He has received 35 patents.

Modeling Resonator Frequency Fluctuations Induced by Adsorbing and Desorbing Surface Molecules.

Y-K Yong[1] and John R. Vig[2]

1) Dept. of Civil and Environmental Engineering
Rutgers University
P.O. Box 909
Piscataway, NJ 08855–0909
(908) 932–3219

2) US Army Electronics Technology and Devices Laboratory
Attn:SLCET-EQ
Fort Monmouth, NJ 07703
(201) 544–4275

Abstract

Resonator frequency fluctuations due to adsorption and desorption of molecules on plate electrodes are studied using the principle of mass-loading effects of adsorbed molecules. The study is based on a 525 MHz, AT-cut quartz resonator enclosed in a small crystal holder. The maximum root mean square of pressure fluctuations at 300 K in a crystal holder with a height and diameter of respectively 1 mm and 2mm is estimated to be in the order 10^{-6} torr, and hence would be a factor in frequency fluctuations if the crystal holder pressure is of the same order of magnitude. Equations relating the surface adsorption rates of crystal holder to pressure are derived, and found to be quadratic polynomial functions of the adsorption rates. Calculations based on these equations show that a contaminant gas with a higher desorption energy creates larger changes in pressure when the temperature is varied. The function describing the frequency fluctuations due to any one contaminant site is a continuous-time Markoff chain. Kolmogoroff equations and an autocorrelation function for the Markoff chain are derived. The autocorrelation, and spectral density function of resonator frequency fluctuations are derived. The spectral density of frequency fluctuations at 1 Hz is studied as a function of pressure, temperature, and desorption energy of molecules. The noise levels for a contaminant gas with one type of molecules are found to be lower for lower desorption energies, and higher at lower pressures. Graphs of the power spectral density functions yield power-law noise processes which range from $1/f^0$ to $1/f^2$. The noise magnitude is sensitive to the composition of the contaminant gas.

I. Introduction.

The effect of a very thin mass layer, such as a monolayer of molecules, on the frequency of a quartz resonator is measurable. This principle is employed in quartz microbalances for surface adsorption studies[1]. Since the molecules adsorbed on the surface are known to have finite lifetimes, the number of adsorbed molecules at a given instant will fluctuate. Hence, short-term frequency instabilities will result if the resonator is sufficiently sensitive to a monolayer of molecules. This was shown to be theoretically possible in ultra-high frequency thickness-shear resonators[2]. The effect may be greater in thin-film resonators where the thickness of the vibrating element, and the size of electrode patch are critical. This paper examines the magnitude and spectral characteristics of frequency fluctuations caused by a contaminant gas of different species of molecules in a simple adsorption-desorption process. The molecules are assumed to adsorb and desorb nondissociatively on the surface electrodes. The adsorbed molecules are also assumed not to exert lateral effects on neighboring adsorbed molecules, nor do they diffuse along the surface. The contaminant gas is confined within a small volume, such as a crystal holder.

II. Dynamic Equilibrium Between the Resonator Surface and the Contaminant Gas.

Due to energy trapping, the mass loading effect of a fluctuating monolayer of molecules is confined almost exclusively to an area within the patch electrodes. The rate of arrival of molecules at the surface can be evaluated readily from simple kinetic theory of gases involving the pressure and kinetic energy of the molecules. If a site spacing of 0.5 nm is assumed, the rates of arrival of different molecules at a site are

$$r_i = 87.8 \times 10^6 P_i / \sqrt{M_i T} \text{ molecules/site/s}, \quad (1)$$

where P_i is the partial pressure in torrs, M_i is the molecular weight of molecules of type i, and T is the temperature in kelvins. Not all the arriving molecules which impinge on the surface stick to it. The rate of contamination of molecules of type i at a site is

$$\lambda_i = s_i r_i \text{ molecules/site/s}, \quad (2)$$

where s_i is the probability of adsorption of arriving molecules of type i at an uncontaminated site. This probability can be measured experimentally. A molecule arriving at a contaminated site is assumed to rebound from the surface.

An adsorbed molecule will reside on a site for a mean time of stay, and subsequently desorb from the surface. The rate of desorption per site is

$$\mu_i = Ae^{-\frac{E_i}{\sqrt{RT}}} \text{ molecules/site/s} \tag{3}$$

where A is assumed to have a value of $1x10^{13}$, E_i is the desorption energy of molecule of type i in kcal/mole, and R is the gas constant. The value of E_i can be measured empirically.

Our derivation of the steady-state probabilities of a site is essentially that given by Langmuir, and discussed in reference [3]. A monolayer or less of adsorbed molecules is assumed. When the system of contaminant gas, and resonator surface settles down to a steady-state dynamic equilibrium, the states of a site, which are either uncontaminated (state 0), or contaminated with a molecule of type i (state i), can be described by steady-state probabilities. The rate at which a site enters state i is equal to the rate at which it leaves, that is,

$$p_0\lambda_i = p_i\mu_i, \tag{4}$$

where the term on the right-hand-side is the leaving rate. The coefficient p_0 is the probability of a site being unoccupied, while p_i is the probability of a site being occupied by a molecule of type i. There are n types of contaminant molecules in the system. Similarly, for state 0,

$$\sum_{i=1}^{n} p_i\mu_i = \sum_{i=1}^{n} p_0\lambda_i, \tag{5}$$

where the right-hand term is the rate at which the site leaves state 0. Since a site must, at any given time, be in one of the states, the steady-state probabilities must sum to one, namely,

$$\sum_{i=0}^{n} p_i = 1. \tag{6}$$

Hence, from Eqs.(4), (5), and (6), we obtain

$$p_0 = \frac{\prod_{j=1}^{n} \mu_j}{\prod_{j=1}^{n} \mu_j + \sum_{j=1}^{n} \left(\lambda_j \prod_{k \neq j}^{n} \mu_k \right)} \tag{7}$$

$$p_i = \frac{\lambda_i \prod_{k\neq i}^{n} \mu_k}{\prod_{j=1}^{n} \mu_j + \sum_{j=1}^{n} \left(\lambda_j \prod_{k\neq j}^{n} \mu_k \right)} \tag{8}$$

$$\text{where } \prod_{j=1}^{n} \mu_j = \mu_1 . \mu_2, \ldots, \mu_{n-1} . \mu_n \ , \tag{9}$$

$$\prod_{k\neq j}^{n} \mu_k = \mu_1 . \mu_2, \ldots, \mu_{j-1} . \mu_{j+1}, \ldots, \mu_{n-1} . \mu_n \text{ if n } \geq 2, \tag{10}$$

$$\text{and } \prod_{k\neq j}^{n} \mu_k = 1 \text{ if n} = 1. \tag{11}$$

The steady-state probability of state 0, p_0, can be interpreted as the fraction of the area which is uncontaminated, while p_i is the fraction of the area contaminated with moelcules of type i.

II. Effects of Fluctuating Pressure on Frequency Fluctuations Caused by Adsorbing and Desorbing Molecules.

We consider the magnitude of pressure fluctuations in a small crystal holder such as the HC-18, with an assumed volume and surface area of 0.475 ml and 475 mm^2, respectively. The pressure increase due to one molecule at 300 K is

$$\Delta_P = \frac{RTn_A}{V} = \frac{62.359 \times 300 \times 6.02 \times 10^{-23}}{0.000475} = 6.54 \times 10^{-17} \text{ torr.} \tag{12}$$

If the adsorption sites are assumed to have a linear dimension of 0.5 nm, the interior surface area of the crystal holder would yield N=1.9x10^{15} adsorption sites. At any given temperature, there is a dynamic equilibrium in the number of molecules adsorbing on, and desorbing from the surface. If we further assume that the adsorption and desorption rates are λ_1 and μ_1, respectively, a Lorentzian type of autocorrelation function for pressure fluctuations is obtained, namely,

$$R_{\Delta p}(t) = \sigma^2 e^{-(\lambda_1+\mu_1)t},$$
$$\text{where } \sigma^2 = N(\Delta p)^2 \frac{\lambda_1 \mu_1}{(\lambda_1 + \mu_1)^2} \tag{13}$$

is the mean square pressure fluctuation. The maximum value of the term

$$\frac{\lambda_1 \mu_1}{(\lambda_1 + \mu_1)^2} \tag{14}$$

is 0.5, hence, the maximum root mean square pressure fluctuation is 2.02×10^{-9} torr. If the ambient pressure is, say, 1 millitorr, the root mean square pressure fluctuation is still six orders of magnitude smaller, and hence would not be a factor in the resonator frequency fluctuations. If the normal pressure in the HC-18 crystal holder at 300 K is as low as 10^{-6} torr, the root mean square pressure fluctuation is still three orders of magnitude smaller.

The pressure fluctuations would be larger in crystal holders smaller than the HC-18. Consider, for example, a 2 mm diameter crystal holder with a height of 1 mm, which we will refer to as "HC-A" in our discussions: The enclosed volume and surface area are approximately 3.14 mm^3, and 14.1 mm^2, respectively. Using (12), the pressure increase due to one molecule at 300 K would be 3.59×10^{-13} torr. The number of sites is 5.64×10^{13}. Hence, the maximum root mean square pressure fluctuation from (13) and (14) is 1.91×10^{-6} torr. This value is about three orders of magnitude larger than in the HC-18 crystal holder. The pressure fluctuations would be a factor if the magnitude of enclosed pressure is of the order 10^{-6} torr.

III. Pressure in a Small Crystal Holder.

Due to outgassing and adsorption, the number of free flying molecules in the confined volume of a small crystal holder varies with temperature. Consider n types of molecules with different molecular weights in the gas enclosed within the crystal holder. The rate of contamination of molecules at an uncontaminated site is from (1), and (2)

$$\lambda_i = q_i P_i, \text{ where } q_i = 87.8 \times 10^6 s_i / \sqrt{M_i T}. \tag{15}$$

From the universal gas law, the partial pressures in the crystal holder are

$$\begin{aligned} P_i &= \frac{N_i RT}{V} = N_i Q, \\ \text{where } Q &= \frac{RT}{V}, \end{aligned} \tag{16}$$

and N_i is the number of moles of molecules of type i in the gas. If the temperature is changed from a reference temperature T_0, there is a change in the number of

free flying molecules which is accommodated in the term N_i. Hence, the partial pressures change accordingly to

$$P_i = \left(N_i^0 + S\left(p_i^0 - p_i\right)\right) Q, \tag{17}$$

where the superscript 0 indicates the state at reference temperature, and S is the number of moles of contamination sites. We subsitute the partial pressures, P_i, of (15) with (17), and employing (8), to yield

$$\lambda_i = q_i \left[N_i^0 + S \left(p_i^0 - \frac{\lambda_i \prod_{k \neq i}^{n} \mu_k}{\prod_{j=1}^{n} \mu_j + \sum_{j=1}^{n} \left(\lambda_j \prod_{k \neq j}^{n} \mu_k \right)} \right) \right] Q, \tag{18}$$

which are quadratic polynomial functions of λ_i. If there are n types of molecules in the system, (18) represents a system of n quadratic equations that the adsorption rates, λ_i, must satisfy simultaneously. The system of equations must be solved numerically. However, if n=1, there is an exact solution

$$\begin{gathered} \lambda_1 = \frac{-B \pm \sqrt{B^2 - 4C}}{2}, \\ \text{where } B = \left(\mu_1 + q_1 Q \left\{ S\left[1 - p_1^0\right] - N_1^0 \right\}\right), \\ \text{and } C = \mu_1 q_1 Q \left(S p_1^0 + N_1^0\right). \end{gathered} \tag{19}$$

There are two roots, one of which is negative and not meaningful. The positive root gives the adsorption rate at the new temperature T. Using the new values of λ_i, and (15), one can obtain the new partial pressures.

We perform some calculations for the "HC-A" and HC-18 crystal holder of the previous section. The volume of the crystal holder changes with temperature, namely,

$$V = V_0 \left(1 + \alpha \left[T - T_0\right]\right)^3 \tag{20}$$

where α is the coefficient of thermal expansion of the steel in the crystal holder, and has a value of 13.3×10^{-6}/C. The values of S for the two holders are 9.35×10^{-11}, and 3.15×10^{-9} moles, respectively. Some results of the pressure of "HC-A" with one type of molecules are shown in Fig.1, where the molecular weight, sticking probability, and reference pressure at 25 C are assigned values of 28, 0.1, and

$1x10^{-5}$ torr, respectively. Five curves are shown, each exhibiting the pressure as a function of temperature for different values of desorption energy, E_1. We observe that when the desorption energy is small, say $E_1<9$ kcal/mol, the system behaves as if there is no adsorption/desorption process, and the number of free-flying molecules remain relatively constant with temperature. Pressure increase of orders of magnitude, due to outgassing, is evident only for a gas with larger desorption energies, say $E_1>18$ kcal/mol. Our calculations also indicate that when the initial pressure is greater than 1 torr, the pressure becomes almost insensitive to the desorption energy of contaminant molecules.

Figure 2 shows the results for the HC-18 crystal holder with a gas system consisting of five types of molecules, each having a molecular weight of, respectively, 32, 28, 16, 44, and 18 (O_2, N_2, CH_4, CO_2, and H_2O). Their desorption energies are respectively assigned values of 9, 12, 15, 18, and 21 kcal/mol. Their sticking probabilities, and partial pressures at 25 C are all given a value of 0.1, and $2x10^{-6}$ torr. The total pressure at 25 C is, hence, $1x10^{-5}$ torr. We observe from Fig.2 that the pressure increase at temperatures above 25 C are principally due to outgassing of molecules with higher desorption energies. The relatively constant pressure at temperatures below 25 C are due mostly to gasses with low desorption energies. The composition of the gas changes with temperature: At temperatures above 25 C, the gas has a higher percentage of molecules with higher desorption energies. The converse is true at temperatures below 25 C. The results discussed in this section are empirically well known.

IV. Frequency Fluctuations Caused by Adsorbing and Desorbing Molecules in a Crystal Holder.

(a) Continuous-Time Markoff Chain for the Frequency Effect of a Site, and Kolmogorov's Backward Equations.

The magnitude of frequency change for a monolayer of mass loading, of which the mass per unit area is much smaller than the mass per unit area of resonator, is

$$\Delta F_i = f_0 \frac{m_i}{m}, \tag{21}$$

where f_0 is the resonator frequency, m_i is the mass per unit area of a monolayer of molecules of type i, and m is the mass per unit area of resonator. Plane waves

along the thickness axis were assumed. If there N_r molecules in the monolayer, the magnitude of frequency change per site due to molecule of type i is

$$a_i = \frac{\Delta F_i}{N_r}. \tag{22}$$

The magnitude of thickness shear vibrations is maximum at the center of resonator with the vibrations decaying to zero near the edges of electrode. This implies that the mass loading effect of the monolayer is exerted predominantly by contaminant molecules located near the center of electrode. Hence the effective N_r value is smaller than that given in (22) which leads to larger values of a_i. The plane wave assumption is conservative, and is employed for the sake of simplicity in our derivations.

The frequency effect $f_k(t)$ of a contaminant site k, in the process of adsorbing or desorbing a molecule, is a continuous-time Markoff chain with a time record given by

$$\begin{aligned} f_k(t) = a_0 = 0 \text{ if site k is unoccupied, and} \\ f_k(t) = a_i \text{ if site k is occupied by a molecule of type i,} \end{aligned} \tag{23}$$

Figure 3 shows a typical time record of $f_k(t)$. The length of time a site remains at a certain state is an exponential random variable with a rate that is state dependent. For example, if site k is occupied by a molecule of type i, the length of time the site remains at state i is an exponential random variable with a rate equal to the molecule desorption rate.

We define a conditional probability function $P_{ij}(t)$, which is also shown in Fig.3, as the probability that $f_k(t) = a_j$ given that $f_k(0) = a_i$, that is,

$$P_{ij}(t) = P\{f_k(t) = a_j \mid f_k(0) = a_i\} \quad \text{i,j=0,1,...,n} \tag{24}$$

Since the molecules adsorb on the sites independently, the rate of adsorption at site k, ν_0, is the sum of the rates of adsorption of molecule of type i, that is,

$$\nu_0 = \sum_{i=1}^{n} \lambda_i. \tag{25}$$

The rate of desorption from the site, ν_i, is dependent on the type of molecule adsorbed, namely,

$$\nu_i = \mu_i, \text{ i=1,2,...,n.} \tag{26}$$

The state of site k goes through sequential cycles of adsorption, and desorption at rates given by (25), and (26). The probability that an adsorbing molecule is of type i when the site goes through a transition from being empty to an occupied state i is

$$\pi_{0i} = \frac{\lambda_i}{\sum_{j=1}^{n} \lambda_j}, \tag{27}$$

where π_{0i} represents the transition probability from state 0 to state i. The transition probability from state i to state 0 is one

$$\pi_{i0} = 1. \tag{28}$$

Equations (27), and (28) cover all the possible transitions; hence, all other transition probabilities are zero

$$\pi_{ij} = 0 \text{ for } i \neq j \; i,j = 1,2,...,n. \tag{29}$$

The conditional probability function $P_{ij}(t)$ of the continuous-time Markoff chain can be shown to satisfy a system of first order, homogeneous, differential equations known as the Kolmogorov's backward equations[4]

$$\frac{d(P_{ij}(t))}{dt} = \nu_i \sum_{k \neq i}^{n} \pi_{ik} P_{kj}(t) - \nu_i P_{ij}(t), \; i,j = 0,1,...,n, \tag{30}$$

which, employing (25) to (29), can be written in the matrix form

$$\frac{d\mathbf{P}(t)}{dt} = \mathbf{\Lambda P} \tag{31}$$

$$\text{where } \mathbf{P} = \begin{bmatrix} P_{00}(t) & P_{01}(t) & ... & P_{0n}(t) \\ P_{10}(t) & P_{11}(t) & ... & P_{1n}(t) \\ ... & ... & ... & ... \\ P_{n0}(t) & P_{n1}(t) & ... & P_{nn}(t) \end{bmatrix}, \tag{32}$$

$$\text{and } \Lambda = \begin{bmatrix} -\sum_{i=1}^{n} \lambda_i & \lambda_1 & \lambda_2 & \dots & \lambda_n \\ \mu_1 & -\mu_1 & 0 & \dots & 0 \\ \mu_2 & 0 & -\mu_2 & \dots & 0 \\ \dots & \dots & \dots & \dots & \dots \\ \mu_n & 0 & 0 & \dots & -\mu_n \end{bmatrix}. \tag{33}$$

Since there is no transition when the elapsed time t is zero, the initial conditions **P**(0) for (31) form an identity matrix. The Kolmogorov's backward equations can be solved[5] to yield

$$\mathbf{P}(t) = \mathbf{VEV^{-1}}, \tag{34}$$

where **V** is a matrix whose column vectors are the eigenvectors of Λ in (33), and

$$\mathbf{E}(t) = \begin{bmatrix} e^{-\beta_0 t} & 0 & \dots & 0 \\ 0 & e^{-\beta_1 t} & \dots & 0 \\ \dots & \dots & \dots & \dots \\ 0 & 0 & \dots & e^{-\beta_n t} \end{bmatrix}. \tag{35}$$

where terms β_i (i=0,1,2,...,n) are the eigenvalues of Λ. Since Λ is singular, a zero eigenvalue always exists, and we can define β_0 equal to zero. The matrix of conditional probabilities **P**(t) are functions of elapsed time t arising from the exponential time functions in **E**(t).

(b) Autocorrelation Function, and Spectral Density Function of Resonator Frequency Fluctuations.

The autocorrelation function of the continuous-time Markoff chain $f_k(t)$ in (23) is defined as the expected value of the product of $f_k(t)$, and $f_k(0)$, that is,

$$R_{f_k}(t) = E_k\left[f_k(t)\, f_k(0)\right]. \tag{36}$$

Using the definition of an expected value[4], we can write (36) as

$$R_{f_k}(t) = \sum_{i=0}^{n}\sum_{j=0}^{n} a_i a_j P\left\{f_k(t) = a_j, f_k(0) = a_i\right\}. \tag{37}$$

where the term $P\{f_k(t)=a_j,\ f_k(0)=a_i\}$ is the joint probability function of $f_k(t)$ and $f_k(0)$. The joint probability function can be calculated by employing the

conditional probabilities in (34), and steady-state probabilities in (7) and (8), namely,

$$P\{f_k(t) = a_j, f_k(0) = a_i\} = P_{ij}(t)\, p_i. \tag{38}$$

Hence, (37) can be written as

$$R_{f_k}(t) = \sum_{i=0}^{n} \sum_{j=0}^{n} a_i a_j P_{ij} p_i. \tag{39}$$

The resonator frequency change is the algebraic sum of the frequency effects of all contaminant sites on the two surfaces of quartz plate, which can be expressed as

$$F(t) = \sum_{k=1}^{2N_r} f_k(t). \tag{40}$$

The autocorrelation function of the resonator frequency change is, by definition, the expected value of the product of F(t) and F(0), that is,

$$R_F(t) = E[F(t)\, F(0)]. \tag{41}$$

When F(t) and F(0) in (41) are substituted by the relation in (40), we obtain

$$R_F(t) = E\left[\sum_{k=1}^{2N_r} f_k(t) \sum_{l=1}^{2N_r} f_l(0)\right]. \tag{42}$$

Since the effects of contaminant sites are mutually independent, the expected values of cross product terms are zero; and (42) is simplified to

$$R_F(t) = \sum_{k=1}^{2N_r} E_k[f_k(t)\, f_k(0)]. \tag{43}$$

The coefficients on the right-hand side of (43) are autocorrelation functions of frequency effects due to site k; therefore, using the expression in (36),

$$R_F(t) = \sum_{k=1}^{2N_r} R_{f_k}(t). \tag{44}$$

We note that the generic site k is indistinguishable from other sites on the surfaces, hence, we can further simplify (44) to

$$R_F(t) = 2N_r R_{f_k}(t). \tag{45}$$

The relation for the autocorrelation function of site k is given in (39), hence,

$$R_F(t) = 2N_r \sum_{i=0}^{n} \sum_{j=0}^{n} a_i a_j P_{ij}(t)\, p_i. \tag{46}$$

We substitute the term $P_{ij}(t)$ by (34), and rewrite (46) as

$$R_F(t) = \sum_{i=0}^{n} \sigma_i^2 e^{-\beta_i t}, \tag{47}$$

$$\text{where } \sigma_i^2 = \sum_{k=0}^{n} \sum_{l=0}^{n} 2N_r a_k a_l v_{ki} w_{il} p_k \tag{48}$$

The coefficients v_{ki}, and w_{il} are the matrix elements of V, and V^{-1}, respectively. We observe that the autocorrelation function in (47) is made up of a sum of (n+1) Lorentzian autocorrelation functions. Each site has (n+1) states. We can now see that the reciprocals of eigenvalues β_i are the correlation times of the autocorrelation function. The terms σ_i^2 are the mean square frequency fluctuations, except for σ_0^2 which is associated with the zero eigenvalue, β_0. The term σ_0^2 represents a constant dc term in the noise process, and is $2N_r$ times the square of mean frequency fluctuations of one site. When it is removed from $R_F(t)$ in (47), we obtain the autocorrelation function of frequency fluctuations about a mean frequency,

$$R_{\Delta F}(t) = \sum_{i=1}^{n} \sigma_i^2 e^{-\beta_i t}, \tag{49}$$

We substitute (22) into (48), noting that $a_0=0$, to obtain the mean square frequency fluctuations in terms of ΔF_i, namely,

$$\sigma_i^2 = \sum_{k=1}^{n} \sum_{l=1}^{n} 2 \frac{\Delta F_k \Delta F_l}{N_r} v_{ki} w_{il} p_k \tag{50}$$

Most noise measurements are made in terms of the spectral density of frequency or phase fluctuations. In the present work, we take the Fourier transform of the autocorrelation function in (49), and use Wiener-Khintchine relation to obtain the one-sided spectral density of frequency fluctuations $S_{\Delta F}$(f):

$$S_{\Delta F}(f) = \sum_{i=1}^{n} \frac{4\sigma_i^2 \beta_i}{\left(\beta_i^2 + 4\pi^2 f^2\right)}, \tag{51}$$

where f is the Fourier frequency. (49), and (51) reveal all the essential information about the resonator frequency fluctuations induced by the adsorption and desorption of n species of molecules. They are similar to (22), and (23) of reference [2], which were derived for one species of molecules. The magnitude of spectral density is proportional to the square of ΔF_i, which is the mass loading effect of a monolayer of molecules of type i; and inversely proportional to N_r. The magnitude of N_r depends on the size of electrode patch, and contaminant site spacing. The spectral density function given by (51) is a superposition of n number of Lorentzian spectra with a distribution of corner frequencies β_i given by the eigenvalues of (33). Our model has characteristics similar to that given by McWhorter[6]. Over a certain range of Fourier frequencies, 1/f noise can be generated if β_i is uniformly distributed, having at least one corner frequency per decade of Fourier frequency[7], and an associated variance, σ_i^2, which is of significant magnitude.

The spectral density of frequency fluctuations at 1 Hz is useful for comparing data of noise magnitudes resulting from different initial pressures, temperatures, and types of molecules, and is obtained from (51) by setting f equal to one,

$$S_{\Delta F}(1) = \sum_{i=1}^{n} \frac{4\sigma_i^2 \beta_i}{\left(\beta_i^2 + 4\pi^2\right)}. \tag{52}$$

V. Noise Calculations for a 525 MHz, UHF AT-cut Quartz Resonator.

The fundamental frequency limitations imposed by conventional lapping and polishing methods can be overcome by the application of chemical polishing techniques[8]. The feasibility of producing above-500 MHz fundamental mode resonators has been demonstrated[9]. We consider a 525 MHz AT-cut resonator with an electrode area of 0.003mm^2, and thickness of 3.2 μm. The resonator is

confined within the "HC-A" crystal holder, and pressure fluctuations are neglected. If we assume the contaminant sites on the plate electrodes have a linear dimension of 0.5 nm, then the value of N_r is $12x10^9$ sites. The frequency change for a 0.5 nm monolayer of molecules with a density equal to that of quartz is, from (21),

$$\Delta F = f_0 \frac{m'}{m} = 82 \text{ KHz}, \tag{53}$$

where f_0 is 525 MHz. Since the values of molecular weights to be considered are all of the same order of magnitude, we simplify the calculations by setting ΔF_i (i=1,2,3,4,5) to that given in (53).

Figure 4 shows the spectral density of frequency fluctuations at 1 Hz as a function of temperature for a contaminant gas with one type of molecules. Four curves are exhibited for desorption energies ranging from 9 to 18 kcal/mole. The pressure in crystal holder as a function of temperature is obtained from the pressures curves of Fig.1. The initial pressure at 25 C is $1x10^{-5}$ torr. We observe that in general the noise levels are higher for molecules with higher desorption energies. For temperatures above 30 C, a gas having a desorption energy of 18 kcal/mol. exhibits spectral densities of frequency fluctuations at 1 Hz which are more than ten orders of magnitude greater one with a desorption energy of 9 kcal/mol.

A series of simulations is performed to study the characteristics of spectral density of frequency fluctuations given by (51). Spencer and Smith[10] performed a spectrometric analysis of residual gases in metal enclosures, and found predominant gases such as nitrogen, carbon dioxide, and oxygen, and traces of methane, and water.

Values of the sticking probabilities, and desorption energies are needed in order to calculate the rates of adsorption, and desorption. Accurate values of desorption energies of contaminant gases in quartz resonators are generally not available. Water has desorption energies between 22, and 24 kcal/mole on metal surfaces[11]. The sticking probability is sensitively dependent on the gas-metal system, the values of which span the range $10^{-7} \leq s_i \leq 1$. For hydrogen, oxygen, carbon monoxide, and nitrogen molecules on metals, and at substrate temperatures where chemisorption does occur, the sticking probabilities[12] are generally between 0.1, and 1. We assume for our simulations a sticking probability of 0.1, and desorption energies of 14.0, 15.5, 17.0, 18.5, and 20.0 kcal/mole for oxygen, nitrogen, methane, carbon dioxide, and water molecules, respectively.

There are no compelling reasons for choosing these values other than for the purpose of estimating the magnitude, and characteristics of the noise process. The following table shows the total pressures, and partial pressures for six simulations numbered S1 to S6. The percent total pressure for simulations S1, S2, and S3 are chosen from Spencer and Smith's[8] data on one crystal unit. Simulations S1 to S3 will show the effects of total pressure of a contaminant gas mixture with a fixed composition. Simulations S4 to S6 attempt to show the effects of varying composition of the contaminant gas mixture.

Simulation number	Total pressure at 25 C (torr)	% total pressure				
		Oxygen	Nitrogen	Methane	Carbon dioxide	Water
S1	1E-5	5.3	77.7	0.7	15.6	0.7
S2	1E-3	5.3	77.7	0.7	15.6	0.7
S3	1E-1	5.3	77.7	0.7	15.6	0.7
S4	1E-3	20.0	20.0	20.0	20.0	20.0
S5	1E-3	95.0	1.25	1.25	1.25	1.25
S6	1E-3	1.25	1.25	1.25	1.25	95.0

Figure 5 exhibits the spectral density of frequency fluctuations curves for simulations S1, S2, and S3. We observe that the frequency fluctuations do not follow a simple power law noise process: the slope of spectral density curves range from $1/f^0$ to $1/f^2$. The difference in total pressure between simulations S1, and S3 is four orders of magnitude, while their spectral densities generally differ by about an order of magnitude. In Fig.6, we observe that by changing the composition of the gas according to the values given in the table, which are all within the same order of magnitude, the spectral densities can change as much as two orders of magnitude. Hence, it seems that the noise process is more sensitive to the composition of contaminant gas than to total pressure.

Acknowledgement

This work was supported by the U.S. Army Research Office, contract no. DAAL03–87–K-0107.

References

1. Lu, C., and Czanderna, A.W., /Editors, Applications of Piezoelectric Quartz Crystal Microbalances, Methods and Phenomena, Their Applications in Science and Technology, Vol.7, Elsevier (Amsterdam), 1984.
2. Yong, Y-K, and Vig, J.R., "Resonator Surface Contamination – A Cause of Frequency Fluctuations?" IEEE Transactions on Ultrasonics ,Ferroelectrics, and Frequency Control, Vol.36, No.4, 1989, pp452–458
3. Adamson, A.W., Physical Chemistry of Surface, 4th edition, John Wiley Press (New York), 1982, pp521–523.
4. Ross, S.M., Introduction to Probability Models, 3rd Edition, Academic Press, Orlando, 1985, chapter 6.
5. Potter, M.C., and Goldberg, J., Mathematical Methods, 2nd Edition, Prentice-Hall, Englewood Cliffs, 1987, pp293–295.
6. McWhorter, A.L.,"1/f Noise and Germanium Surface Properties," Semiconductor Surface Physics, edited by R.H. Kingston, 1957, pp207–228.
7. Keshner, M.S., "1/f Noise," Proceedings of the IEEE, Vol.70, N0.3, March 1982, pp212–218.
8. Vig, J.R., Lebus, J.W., and Filler, R.L., "Chemically Polished Quartz," Proceedings of the 31st Annual Symposium on Frequency Control, 1977, pp131–143.
9. Hunt, J.R., and Smythe, R.C., "Chemically Milled VHF and UHF AT-cut Resonators," Proceedings of the 39th Annual Symposium on Frequency Control, 1985, pp292–300.
10. Spencer, W.J., and Smith, W.L., "Precision Quartz Crystal Controlled Oscillator for Severe Environmental Conditions," Proceedings of the 16th Annual Symposium on Frequency Control, 1962, pp405–421.
11. Maissel, L.I., and Glang, R., /editors, Handbook of Thin Film Technology, McGraw-Hill (New York), 1979, chapter 2, pp44.
12. Morris, M.A., Bowker, M., and King, D.A., "Kinetics of Adsorption, Desorption, and Diffusion at Metal Surfaces," Comprehensive Chemical Kinetics, Simple Processes at the Gas-Solid Interface, Vol.19, edited by C.H. Bamford, et al., Elsevier (Amsterdam), 1984, pp41–55.

List of figures.

Fig.1 Pressure in crystal holder as a function of temperature for a gas with one type of molecules.

Fig.2 Pressure in crystal holder as a function of temperature for a gas with five types of molecules.

Fig.3 Continuous-time Markoff chain, $f_k(t)$, for the frequency effect of a contaminant site. Also shown is the conditional probability function, $P_{ij}(t)$.

Fig.4 Spectral density of frequency fluctuations at 1 Hz as a function of temperature for a contaminant gas consisting of one type of molecules.

Fig.5 Spectral density of frequency fluctuations for simulations S1, S2, and S3.

Fig.6 Spectral density of frequency fluctuations for simulations S4, S5, and S6.

Fig.1 Pressure in crystal holder as a function of temperature for a gas with one type of molecules.

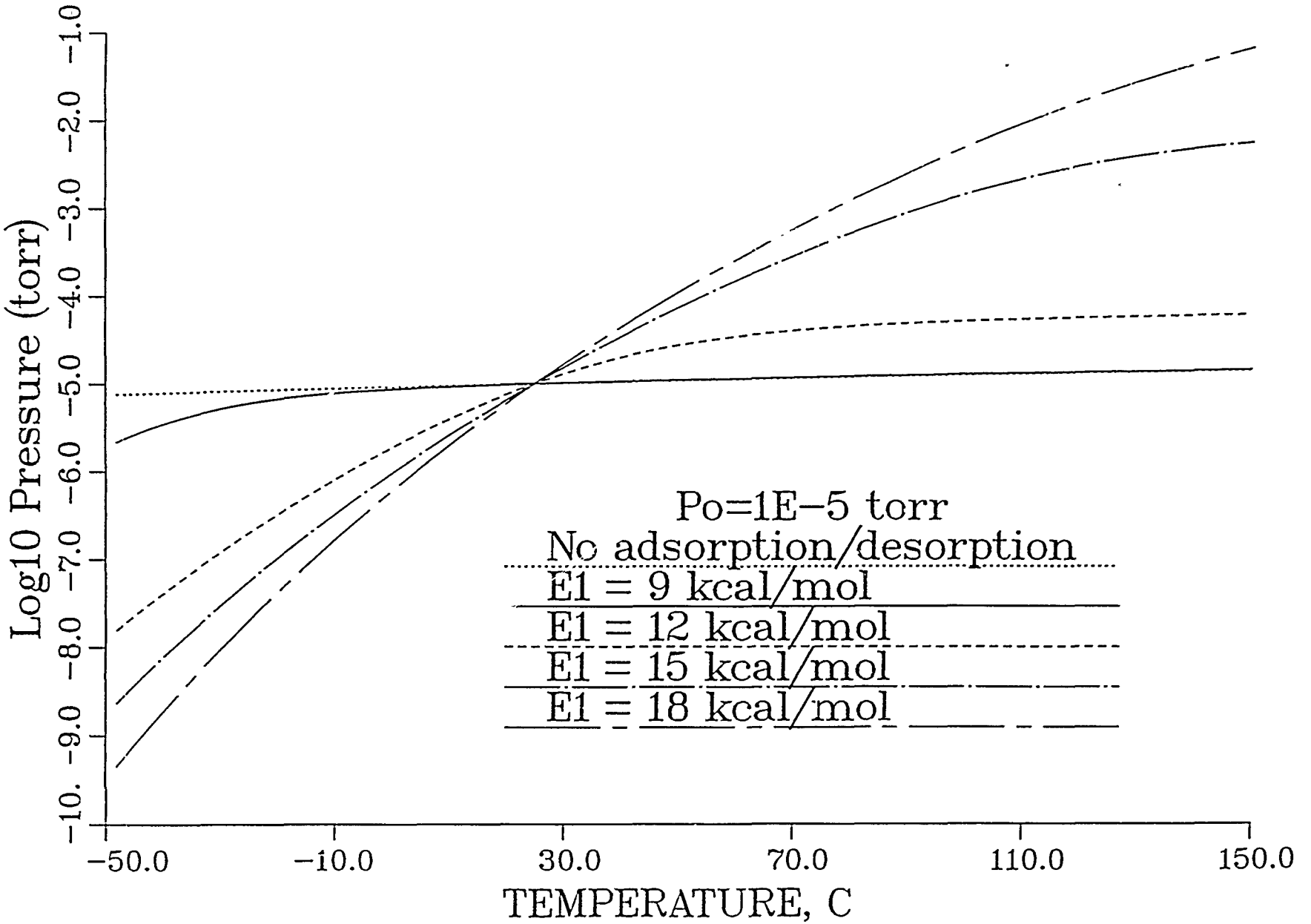

Fig. 2 Pressure in crystal holder as a function of temperature for a gas with five types of molecules.

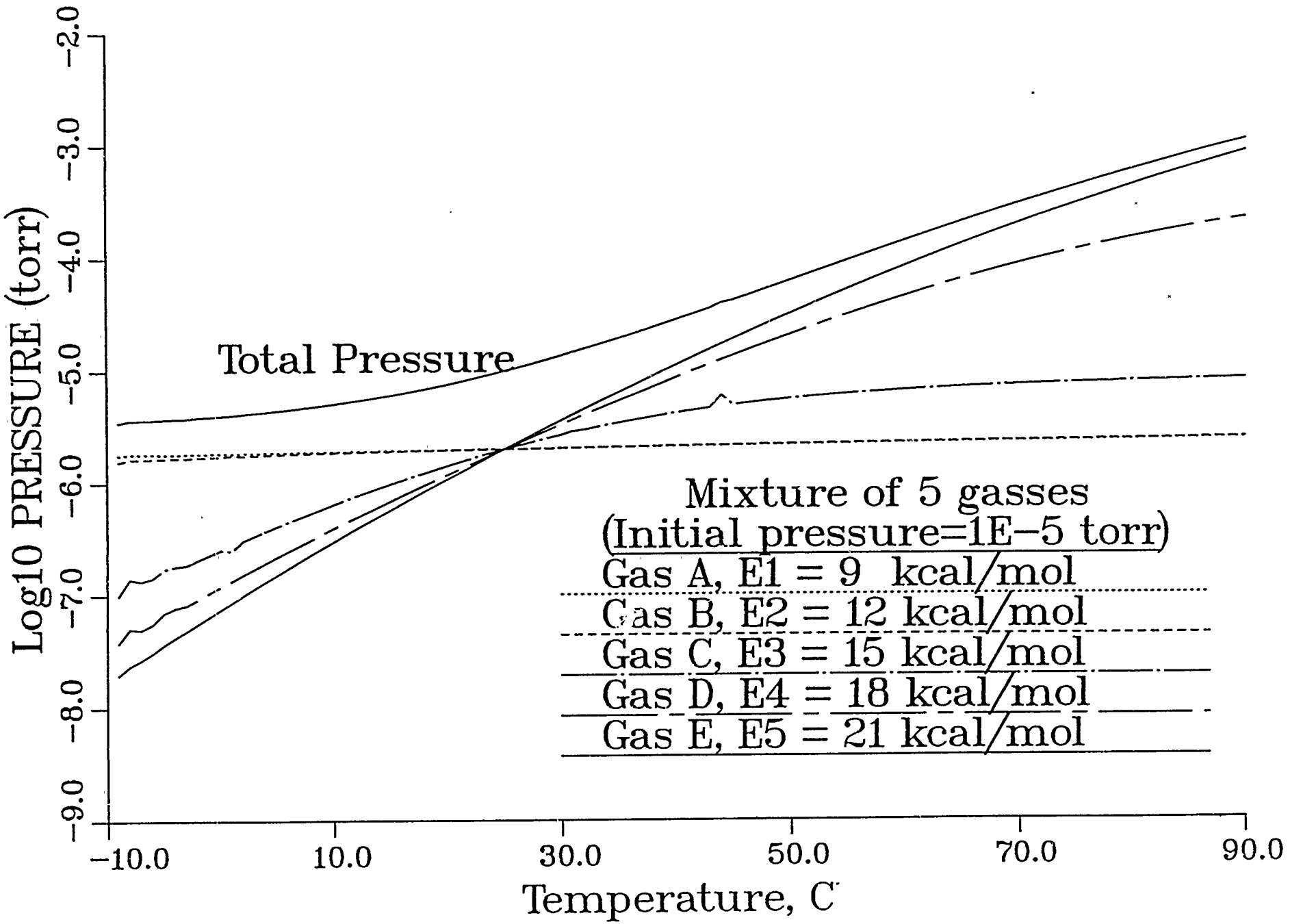

Fig. 3 Continuous-time Markoff chain, $f_k(t)$, for the frequency effect of a contaminant site. Also shown is the conditional probability function, $P_{ij}(t)$.

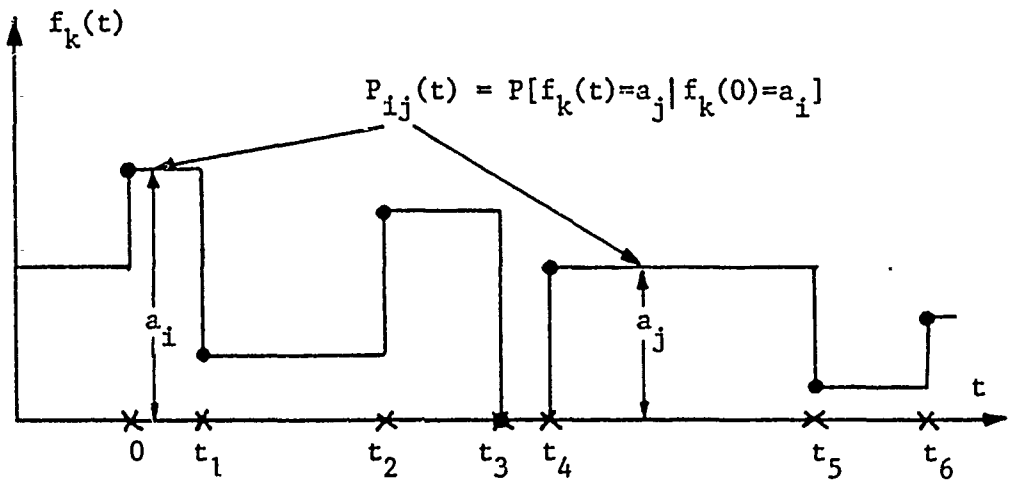

Fig. 4 Spectral density of frequency fluctuations at 1 Hz as a function of temperature for a contaminant gas consisting of one type of molecules.

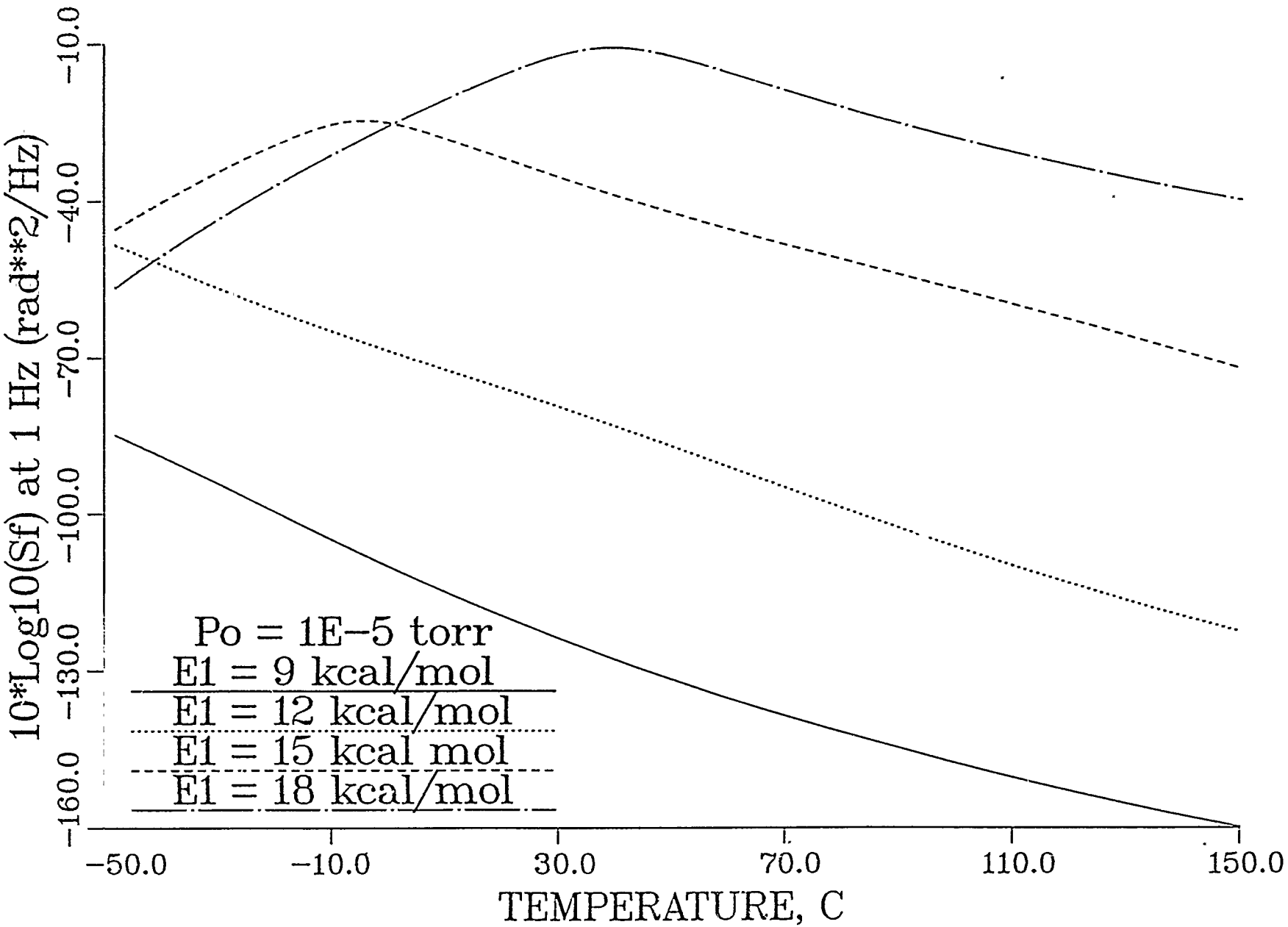

Fig. 5 Spectral density of frequency fluctuations for simulations S1, S2, and S3.

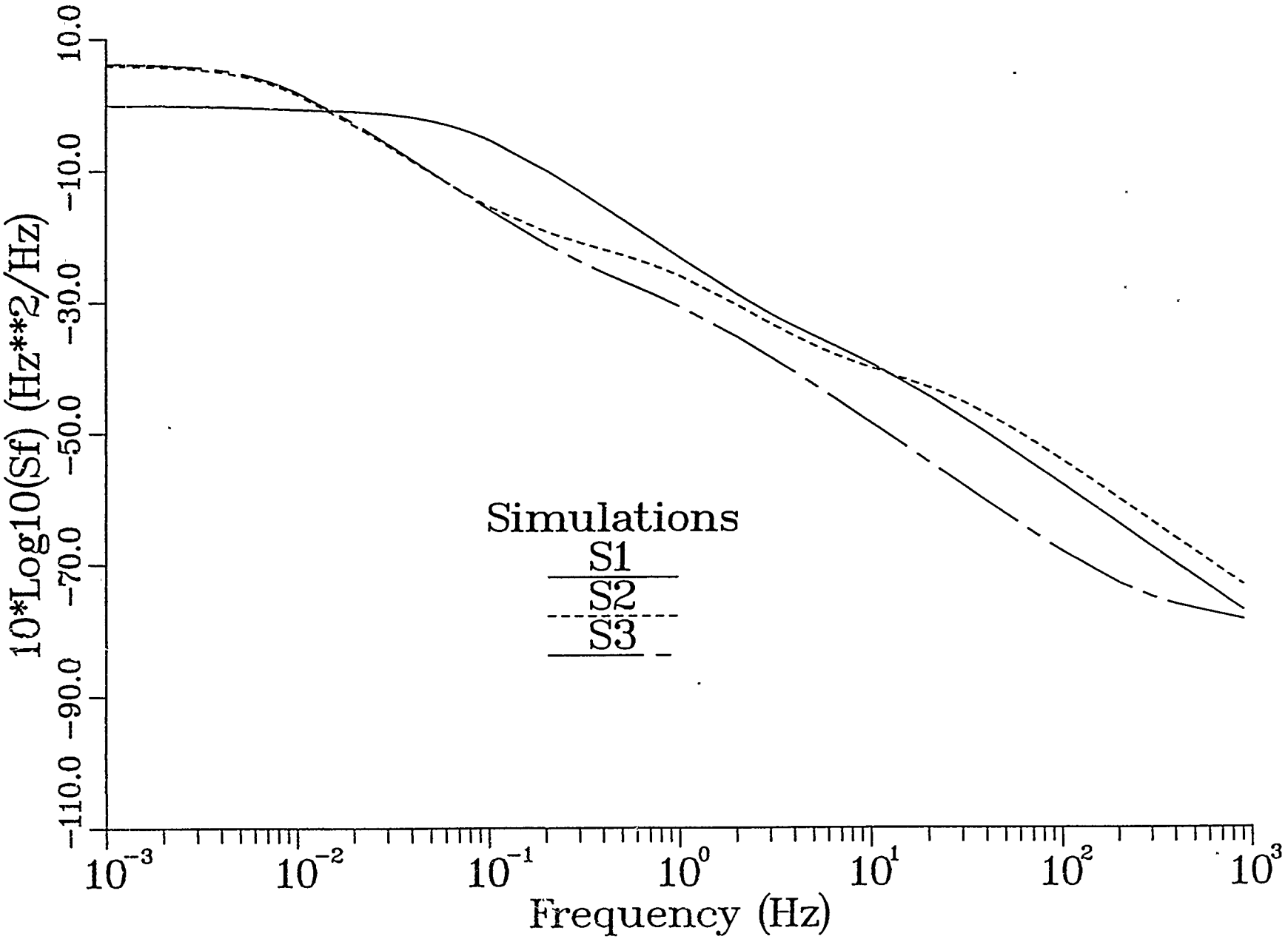

Fig. 6 Spectral density of frequency fluctuations for simulations S4, S5, and S6.

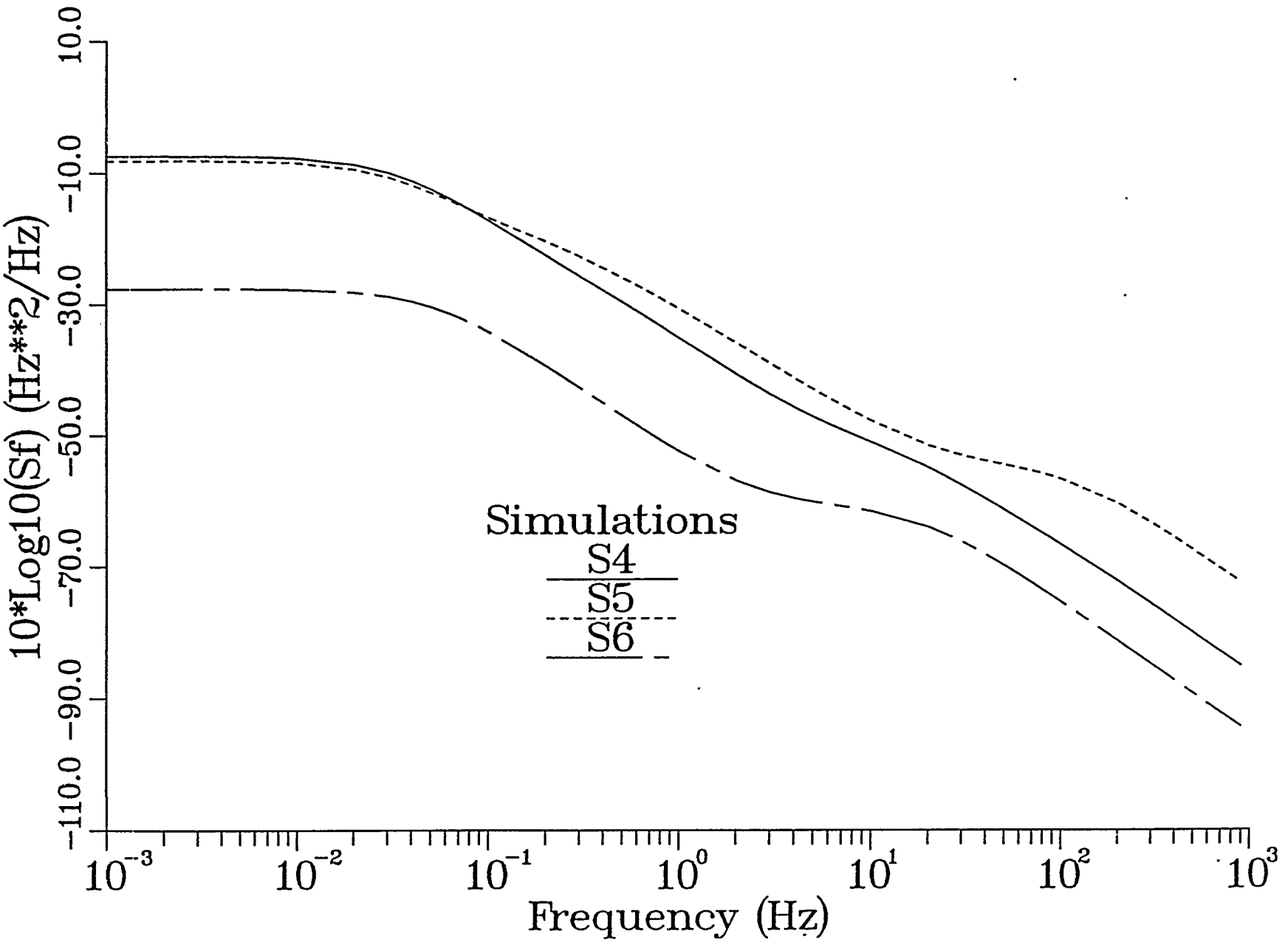

Simulation of Noise Processes in Thickness-Shear Resonators Caused by Multilayer Adsorption and Desorption of Surface Molecules.

Yook-Kong Yong

Dept. of Civil/Environmental Engineering, Rutgers University, P.O. Box 909, Piscataway, NJ 08855–0909

ABSTRACT.

Effects of multilayer contamination on mean resonant frequency and frequency fluctuations in thickness-shear resonators are studied. A model based on mass-loading of contaminant molecules with adsorption and desorption rates is developed. Equations relating change in mean frequency and frequency fluctuations to adsorption and desorption rates are derived. Since the adsorption and desorption rates are functions of pressure and temperature, change in mean frequency and spectral density of frequency fluctuations are studied with respect to pressure and temperature. Calculations are performed for a 10 MHz thickness-shear resonator. Frequency-temperature and frequency-pressure curves are plotted for the 10 MHz resonator. The curves do not follow a cubic polynomial function and have a magnitude in the range of 10 ppm. The mean square of frequency fluctuations under multilayer contamination is significantly greater than that under monolayer contamination. The spectral density of frequency fluctuations at 1 Hz is quite constant in a wide range of temperatures (-50 to 100°C) when the values of heat of adsorption for the second and subsequent layers is close to that for the first layer. The magnitude of spectral density of frequency fluctuations is about –120 dBc (Hz^2/Hz).

I. Introduction.

The effect on resonant frequency due to a very thin mass layer, such as one or more layers of molecules, adsorbed on a thickness-shear quartz resonator is measurable, and is employed in quartz microbalances for surface adsorption studies[1]. Since the adsorbed molecules are known to have finite lifetimes on the surface, the number of adsorbed molecules at a given instant will fluctuate. Hence, short-term frequency instabilities will result if the resonator is sufficiently sensitive to the fluctuations. This was shown to be theoretically possible for monolayer contamination in ultra-high-frequency thickness-shear resonators[2]. We examine in this paper the effects of temperature and pressure on changes in mean resonant frequency and frequency fluctuations due to multilayer adsorption of contaminant molecules on the surfaces of a 10 MHz thickness-shear resonator.

II. Adsorption of Gases and Vapors on a Resonator Surface.

For multilayer adsorption of gases and vapors on the surfaces of a thickness-shear resonator, we employ a BET model which was proposed by Brunauer, Emmett, and Teller[3]. The reader is also referred to a text by Adamson[4]. The assumptions are: (1) The number of molecules adsorbing on a given surface is equal the number of molecules desorbing during a steady state equilibrium, (2) the heat of adsorption for the first layer, E_1, has some special value, whereas for all succeeding layers, it is equal to the heat of condensation of the liquid adsorbate, E_v, and (3) the adsorption and desorption can occur only from or on exposed surfaces. Figure 1 from reference [4] shows portions of surfaces S_i covered by i ($i = 0, 1, 2,...,$) layers of contaminant molecules. The adsorbed molecules are assumed to have no lateral interactions with their neighbors.

a) Adsorption and Desorption Rates of Contaminant Molecules.

The rate of arrival of molecules at a surface can be evaluated readily from simple kinetic theory of gases involving the pressure and kinetic energy of the molecules. If a site spacing of 0.5 nm is assumed, the rate of arrival of molecules at a site is

$$r = 87.8\text{x}10^6 P/\sqrt{MT} \text{ molecules/site/s}, \qquad (1)$$

where P is pressure in torrs, M is molecular weight of molecules, and T is temperature in kelvins. Not all the arriving molecules which impinge on the surface stick to it. The rate of contamination of molecules at a site is

$$\lambda_i = s_i r \text{ molecules/site/s}, \qquad (2)$$

where s_i is the sticking coefficient which is the probability of adsorption of a molecule impinging at the surface S_i.

An adsorbed molecule will reside on a site for a mean time of stay, and subsequently desorb from the surface. The rate of desorption per site from surface S_1 is

$$\mu_1 = Ae^{-E_1/\sqrt{RT}} \text{ molecules/site/s,} \quad (3)$$

where A is assumed to have a value of $1\text{x}10^{13}$, E_1 is the heat of adsorption in kcal/mole, and R is the gas constant. For surfaces S_i where i is greater than one, the rate of desorption per site is

$$\mu_2 = Ae^{-E_v/\sqrt{RT}} \text{ molecules/site/s,} \quad (4)$$

where E_v is the heat of condensation in kcal/mole.

b) Dynamic Equilibrium Between the Resonator Surface and the Contaminant Gas.

The derivation of the steady-state probabilities of a site being uncontaminated, or contaminated with one or more molecules, follows essentially that given by the BET model. We presently assume that the adsorbed mass layer will consists of no more than three layers of molecules. Hence, the sticking coefficient s_3 is given a value of zero. Derivations for models with more than three layers are similar to what is given here. When the system of contaminant gas and resonator surface settles down to a steady state dynamic equilibrium, the states of a site, which is either uncontaminated (state 0), or contaminated with i molecules in a layerwise manner, can be described by steady-state probabilities p_i $(i = 0, 1, 2, 3)$. The rate at which a site enters state i is equal to the rate at which it leaves, that is,

$$\begin{aligned} p_0\lambda_0 &= p_1\mu_1 \\ p_1\lambda_1 &= p_2\mu_2 \\ p_2\lambda_2 &= p_3\mu_2. \end{aligned} \quad (5)$$

The steady-state probabilities must sum to one, since the site must at any given time be in one of the states,

$$p_0 + p_1 + p_2 + p_3 = 1. \quad (6)$$

The steady-state probabilities p_i can be expressed in terms of the adsorption and desorption rates using Eqs.(5) and (6):

$$\begin{aligned} p_0 &= \frac{1}{D} \\ p_1 &= \frac{\lambda_0}{\mu_1 D} \\ p_2 &= \frac{\lambda_0\lambda_1}{\mu_1\mu_2 D} \\ p_3 &= \frac{\lambda_0\lambda_1\lambda_2}{\mu_1\mu_2^2 D} \end{aligned} \quad (7)$$

$$\text{where } D = 1 + \frac{\lambda_0}{\mu_1} + \frac{\lambda_0\lambda_1}{\mu_1\mu_2} + \frac{\lambda_0\lambda_1\lambda_2}{\mu_1\mu_2^2}.$$

III. Changes in Mean Resonant Frequency.

From Eq.(7), we observe that the steady-state probabilities p_i, being functions of the adsorption and desorption rates, are functions of temperature and pressure for a given absorbate-contaminant system. The sensitivity of the resonator to mass loading is confined mainly to the electrode patch. A monolayer of contaminant molecules covering the electrode patch will change the resonant frequency by the amount

$$\Delta_f = -f_0\frac{m'}{m} \quad (8)$$

where m' and m are the mass per unit area of contaminant molecules and mass per unit area of resonator plate, respectively. The resonator frequency is f_0. The negative sign signifies that the resonant frequency decreases with mass loading. Eq.(8) is valid only when the mass per unit area of contaminant molecules is much smaller than the mass per unit area of resonator plate. The resonator is assumed to vibrate in a pure thickness-shear mode. The actual change in frequency will depend on the number of molecular layers and fraction of surface covered, namely,

$$\frac{\Delta f}{f_0} = 2\Delta_f\left((p_1 - p_{1_0}) + 2(p_2 - p_{2_0}) + 3(p_3 - p_{3_0})\right) \quad (9)$$

where p_{i_0} $(i = 1, 2, 3)$ are the steady-state probabilities at the reference temperature and pressure, and the factor 2 on the right hand side accounts for contaminant on the top and bottom surface.

a) Changes in Mean Resonant Frequency for a 10 MHz Thickness-Shear Resonator.

Simple calculations are performed for a 10 MHz thickness-shear resonator to examine the characteristics and magnitude of changes in mean frequency as a function of temperature and pressure. The resonator thickness is 0.165 mm and the area of circular electrode patch is 10 mm^2. A 0.5 nm thick monolayer of molecules covering the top electrode and having a density equivalent to quartz will yield

$$\begin{aligned} &\Delta_f = 30 \text{ Hz,} \\ &\text{or } \frac{\Delta_f}{f_0} = 3 \text{ ppm.} \end{aligned} \quad (10)$$

The molecular weight of contaminant molecules is taken as equal to 28. For our calculations of the adsorption rates, we take values of sticking coefficients s_i $(i = 0, 1, 2)$ equal to 0.1.

Figure 2 shows the effects of surface contamination with temperature on the mean resonator frequency in parts per million. Three frequency-temperature curves are given corresponding to heats of adsorption 15, 18, and 21 kcal/mole. The heats of condensation are taken to be 75 percent of their respective heats of adsorption. The pressure is kept constant at 0.001 torr. We observe that the surface contamination as a function of temperature can cause the mean frequency to change as much as 10 ppm. The f-T curves do not follow a cubic polynomial function. The characteristics and magnitudes of curves will be affected by initial pressures, heats of adsorption and condensation, and sticking coefficients. The mean frequency increases with increasing temperature.

Figure 3 shows the effects of surface contamination with pressure on the mean resonator frequency in parts per million. The three frequency-pressure curves have the same corresponding heats of adsorption and condensation as in Fig.2. The temperature is kept constant at 25°C. We observe that the mean frequency is also sensitive to pressure changes, and is of a higher order function than a cubic polynomial. The mean frequency decreases with increasing pressure.

IV. Theoretical Developments for Frequency Fluctuations.

Although there is a steady-state equilibrium in the adsorption and desorption of contaminant molecules, there are instantaneous fluctuations in the number of adsorbed molecules. Each contaminant site on the electrode patch of a thickness-shear resonator exerts a small but finite mass loading effect on the resonant frequency. Hence, the fluctuations will be manifested in short term frequency instabilities. We investigate the magnitude and spectral characteristics of short term frequency fluctuations as caused by spatial and temporal fluctuations in the number of adsorbed contaminant molecules.

a) Birth and Death Processes.

The stochastic analysis of fluctuations in the adsorption and desorption of contaminant molecules follows the usual developments for birth and death processes[5]. The table below gives the birth(adsorption) and death(desorption) rates which follow from Eqs.(2) to (4):

$$\begin{aligned}
&\text{Birth rate in } S_0 \text{ sites} = \lambda_0 \\
&\text{Birth rate in } S_1 \text{ sites} = \lambda_1 \\
&\text{Birth rate in } S_2 \text{ sites} = \lambda_2 \\
&\text{Death rate in } S_1 \text{ sites} = \\
&\text{Death rate in } S_2 \text{ sites} = , \\
&\text{Death rate in } S_3 \text{ sites} = \mu_2
\end{aligned} \tag{11}$$

The birth and death process is a continuous-time Markov chain which is more generally an exponential model. Hence, the state transition rate for a S_i site is simply the sum of birth and death rates associated with the state of the site, that is,

$$\begin{aligned}
&S_0 \text{ site: } \lambda_0 \\
&S_1 \text{ site: } \lambda_1 + \mu_1 \\
&S_2 \text{ site: } \lambda_2 + \mu_2 \\
&S_3 \text{ site: } \mu_3
\end{aligned} \tag{12}$$

b) Frequency Effect of a site $f_k(t)$.

Since each contamination site, say site k, exerts a finite effect on the resonant frequency, the frequency effect can be described by a continuous function $f_k(t)$ which is a continuous-time Markov chain. The function has specific values depending on the state of site:

$$\begin{aligned}
f_k(t) &= a_0 = 0 \text{ for } S_0 \text{ site,} \\
f_k(t) &= a_1 = \frac{\Delta_f}{N_r} \text{ for } S_1 \text{ site,} \\
f_k(t) &= a_2 = \frac{2\Delta_f}{N_r} \text{ for } S_2 \text{ site,} \\
f_k(t) &= a_3 = \frac{3\Delta_f}{N_r} \text{ for } S_3 \text{ site.}
\end{aligned} \tag{13}$$

where N_r is the number of sites on one electrode patch. The magnitude of thickness-shear vibrations is maximum at the center of electrode patch with the vibrations decaying to zero near the edges of electrode. A graph of the magnitude of thickness-shear vibrations will exhibit a Gaussian profile. This implies that the mass loading effect of the contaminant molecules is exerted predominantly near the center third of electrode. Hence the effective N_r value is smaller than the number of sites in one electrode patch. Subsequent analysis will show that a smaller N_r value leads to larger magnitudes of root-mean-square frequency fluctuations.

c) Conditional Probability Function $P_{ij}(t)$ of $f_k(t)$.

The probability of $f_k(t)$ at a subsequent time t having a value of a_j, given an initial value of a_i at t equal to zero,

is defined by a conditional probability function

$$P_{ij}(t) = P\{f_k(t) = a_j \mid f_k(0) = a_i\} \quad i,j = 0,1,2,3. \tag{14}$$

For a continuous-time Markov chain, Eq.(14) must satisfy Kolmogorov's backward equations which are a system of first order differential equations:

$$\frac{d}{dt}\mathbf{P}(t) = \mathbf{\Lambda P}(t), \tag{15}$$

where $\mathbf{P}(t) =$

$$\begin{bmatrix} P_{00}(t) & P_{01}(t) & P_{02}(t) & P_{03}(t) \\ P_{10}(t) & P_{11}(t) & P_{12}(t) & P_{13}(t) \\ P_{20}(t) & P_{21}(t) & P_{22}(t) & P_{23}(t) \\ P_{30}(t) & P_{31}(t) & P_{32}(t) & P_{33}(t) \end{bmatrix}, \tag{16}$$

and $\mathbf{\Lambda} =$

$$\begin{bmatrix} -\lambda_0 & \lambda_0 & 0 & 0 \\ \mu_1 & -(\lambda_1+\mu_1) & \lambda_1 & 0 \\ 0 & \mu_2 & -(\lambda_2+\mu_2) & \lambda_2 \\ 0 & 0 & \mu_2 & -\mu_2 \end{bmatrix}. \tag{17}$$

The initial conditions for Eq.(15) is an identity matrix since at zero time there are no transitions,

$$\mathbf{P}(0) = \begin{bmatrix} 1 & 0 & 0 & 0 \\ 0 & 1 & 0 & 0 \\ 0 & 0 & 1 & 0 \\ 0 & 0 & 0 & 1 \end{bmatrix}. \tag{18}$$

The Kolmogorov's backward equations can be solved[6] to yield

$$\mathbf{P}(t) = \mathbf{VEV}^{-1} \tag{19}$$

where

$$\mathbf{E}(t) = \begin{bmatrix} e^{-\omega_0 t} & 0 & 0 & 0 \\ 0 & e^{-\omega_1 t} & 0 & 0 \\ 0 & 0 & e^{-\omega_2 t} & 0 \\ 0 & 0 & 0 & e^{-\omega_3 t} \end{bmatrix} \tag{20}$$

is a diagonal matrix of exponential time functions with constants ω_m *(m=0, 1, 2, 3)* which are the absolute values of eigenvalues of $\mathbf{\Lambda}$ in Eq.(17). Since $\mathbf{\Lambda}$ is singular, a zero eigenvalue exists, and we can define ω_0 to be the zero eigenvalue. All the nonzero eigenvalues are negative. The column vectors $\mathbf{v}_m$ of $\mathbf{V}$ and eigenvalues $-\omega_m$ form the eigenpairs $\{-\omega_m, \mathbf{v}_m\}$ of $\mathbf{\Lambda}$. Eq.(19) and (20) show that the matrix of conditional probabilities are exponential functions of elapsed time t, namely,

$$P_{ij}(t) = \sum_{m=0}^{3} v_{im} v_{mj}^{-1} e^{-\omega_m t} \tag{21}$$

where v_{im} and v_{mj}^{-1} are elements of matrices $\mathbf{V}$ and $\mathbf{V}^{-1}$, respectively.

d) Autocorrelation Function of Frequency Fluctuations about Mean Resonant Frequency.

The autocorrelation function of the continuous-time Markov chain $f_k(t)$ in Eq.(13) is defined as the expected value of the product of $f_k(t)$, and $f_k(0)$, that is,

$$R_{f_k}(t) = E[f_k(t) f_k(0)], \tag{22}$$

which by definition can be written as

$$R_{f_k}(t) = \sum_{i=0}^{3}\sum_{j=0}^{3} a_i a_j P\{f_k(t) = a_j, f_k(0) = a_i\}, \tag{23}$$

where the term $P\{f_k(t) = a_j, f_k(0) = a_i\}$ is the joint probability distribution function of $f_k(t)$, and $f_k(0)$. The joint probability distribution function can be calculated by employing the conditional probabilities in Eq.(19), and steady-state probabilities in Eq.(7). Hence,

$$P\{f_k(t) = a_j, f_k(0) = a_i\} = P_{ij}(t)\, p_i. \tag{24}$$

Using Eqs.(24) and (21), Eq.(23) can be written as

$$R_{f_k}(t) = \sum_{m=0}^{3} \sigma_m^2 e^{-\omega_m t} \tag{25}$$

$$\text{where } \sigma_m^2 = \sum_{i=0}^{3}\sum_{j=0}^{3} a_i a_j v_{im} v_{mj}^{-1} p_i. \tag{26}$$

Since ω_0 is the zero eigenvalue, σ_0^2 is a constant dc noise which is the square of mean value of $f_k(t)$. In our study of short term instabilities in frequency, we are interested in frequency fluctuations about a mean resonant frequency. Hence, we define a continuous-time Markov chain of frequency fluctuations

$$\Delta f_k(t) = f_k(t) - \sigma_0 \tag{27}$$

The autocorrelation function of frequency fluctuations about a mean frequency for site k is

$$\begin{aligned} R_{\Delta f_k}(t) &= E[\{\Delta f_k(t)\}\{\Delta f_k(0)\}] \\ &= E[f_k(t) f_k(0)] - \sigma_0^2 \\ &= \sum_{m=1}^{3} \sigma_m^2 e^{-\omega_m t} \end{aligned} \tag{28}$$

Note that since a_0 is equal to zero, Eq.(26) can also be written as

$$\sigma_m^2 = \sum_{i=1}^{3}\sum_{j=1}^{3} a_i a_j v_{im} v_{mj}^{-1} p_i. \tag{29}$$

We observe that the sum of σ_m^2 over $m = 1,2,3$ is the mean square of frequency fluctuations due to site k.

There are $2N_r$ sites in the resonator, which accounts for contamination sites on the top and bottom electrodes. Hence, the resonator frequency fluctuation about a mean frequency at any time t is

$$\Delta F(t) = \sum_{k=1}^{2N_r} \Delta f_k(t), \tag{30}$$

whose autocorrelation function is

$$\begin{aligned} R_{\Delta F}(t) &= E[\Delta F(t)\,\Delta F(0)], \\ &= E\left[\left(\sum_{k=1}^{2N_r} \Delta f_k(t)\right)\left(\sum_{l=1}^{2N_r} \Delta f_l(0)\right)\right]. \\ &= \sum_{k=1}^{2N_r}\sum_{l=1}^{2N_r} E[\{\Delta f_k(t)\}\{\Delta f_l(0)\}] \end{aligned} \tag{31}$$

Since the effects of contaminant sites are mutually independent, the expected values of cross product terms are zero, and Eq.(31) becomes

$$\begin{aligned} R_{\Delta F}(t) &= \sum_{k=1}^{2N_r} E[\{\Delta f_k(t)\}\{\Delta f_k(0)\}] \\ &= \sum_{k=1}^{2N_r} R_{\Delta f_k}(t) \end{aligned} \tag{32}$$

The generic site k is indistinguishable from other sites on the electrode surfaces, therefore, the autocorrelation function in Eq.(32) is

$$R_{\Delta F}(t) = 2N_r R_{\Delta f_k}(t). \tag{33}$$

Using the last equation of Eq.(28), we can write Eq.(33) as

$$\begin{aligned} R_{\Delta F}(t) &= \sum_{m=1}^{3} \bar{\sigma}_m^2 e^{-\omega_m t}, \\ \text{where } \bar{\sigma}_m^2 &= 2N_r\sigma_m^2. \end{aligned} \tag{34}$$

We observe that the autocorrelation function in Eq.(34) is made up of three Lorentzian autocorrelation functions. The reciprocals of ω_m are the correlation times of the autocorrelation function. The term

$$\bar{\sigma} = \sqrt{\sum_{m=1}^{3} \bar{\sigma}_m^2} \tag{35}$$

is the root-mean-square of resonator frequency fluctuations, and from Eqs.(13) and (29),

$$\bar{\sigma} = \frac{\Delta_f}{\sqrt{N_r}}\sqrt{\sum_{m=1}^{3}\sum_{i=1}^{3}\sum_{j=1}^{3} 2ij\,v_{im}v_{mj}^{-1}p_i}. \tag{36}$$

Hence the root-mean-square of frequency fluctuations is proportional to the frequency change of resonator to a monolayer of contaminant molecules, and inversely proportional to the square root of the number of contaminant sites in electrode patch.

e) One-Sided Spectral Density of Frequency Fluctuations about Mean Resonant Frequency.

Wiener-Khintchine relation is employed to obtain the one-sided spectral density of frequency fluctuations from the autocorrelation function of Eq.(34); which yields

$$S_{\Delta F}(f) = \sum_{m=1}^{3} \frac{4\bar{\sigma}_m^2\omega_m}{\omega_m^2 + 4\pi^2 f^2}, \tag{37}$$

where f is the Fourier frequency. Eq.(37) reveals all the essential characteristics of frequency fluctuations induced by multilayer surface contamination. The spectral density function is a superposition of three Lorentzian spectra with a distribution of corner frequencies ω_m. The function is similar to that given by McWhorter[7]. Over a certain range of Fourier frequencies, 1/f noise can be generated if ω_m is uniformly distributed with at least one corner frequency per decade of Fourier frequency[8], and the associated $\bar{\sigma}_m^2$ having a significant magnitude. The magnitude of spectral density is proportional to the square of Δ_f, and inversely proportional to N_r.

V. Noise Calculations for a 10 MHz Thickness-Shear Resonator.

Noise calculations for the 10 MHz thickness-shear resonator previously defined in section III(a) is performed. In addition, an average site spacing of 0.5 nm is assumed for the contaminant sites on electrode patches. Hence, the number of sites in one electrode patch is

$$N_r = 4\text{x}10^{13} \text{ sites.} \tag{38}$$

Calculations for both monolayer and multilayer contaminations are performed. The model for monolayer contamination was previously reported in reference [2], and is actually a specialized case of the present model.

Figure 4 shows the spectral density curves of frequency fluctuations plotted as a function of Fourier frequency. Four curves are shown. The solid curve represents monolayer contamination, while the three other curves are for multilayer contamination using values of heat of condensation E_v which are 0.5, 0.75 and 1.0 of E_l, the heat of absorption with a value of 21 kcal/mole. We observe that

the magnitude of spectral density for E_v greater than 0.75 E_l is about 50 dBc greater than the curve with monolayer contamination. For the particular pressure (0.001 torr), temperature (25°C), and Fourier frequency range of less than 100 Hz, the spectral density curves with E_v less than 0.5 E_l resemble the monolayer curve.

The spectral density of frequency fluctuations at 1 Hz offset is useful for comparing data of noise magnitudes resulting from different initial pressures, temperatures, and heats of absorption and condensation. This is obtain from Eq.(37) by setting f equal to one,

$$S_{\Delta F}(1) = \sum_{m=1}^{3} \frac{4\bar{\sigma}_m^2 \omega_m}{\omega_m^2 + 4\pi^2}. \qquad (39)$$

Figure 5 shows the spectral density of frequency fluctuations at 1 Hz plotted as a function of pressure. We observe that for wide ranges of pressures (10^{-5} to 10 torr) the spectral density with multilayer contamination and $E_v > 0.75E_l$ has a magnitude greater than monolayer contamination. The magnitude difference is greater at higher pressures. The curve with $E_v = 0.5E_l$ follows the monolayer curve up to a pressure of about 0.002 torr, and diverges from it at higher pressures.

Figure 6 shows the spectral density of frequency fluctuations at 1 Hz plotted as a function of temperature. Calculations show that for multilayer contamination with $E_v > 0.9E_l$, the magnitude of spectral density at 1 Hz remains remarkably constant in a wide range of temperature (-50 to 100°C), as opposed to the monolayer curve. With $E_v = 0.75E_l$, the multilayer contamination curve remains constant in a shorter range of temperatures (-50 to 35°C). The curve with $E_v = 0.5E_l$ follows the monolayer curve in temperatures greater than 10°C.

VI. Summary.

A model based on mass-loading of contaminant molecules having adsorption and desorption rates is developed. Calculations are made for a 10 MHz thickness-shear resonator. The model brings out some interesting aspects of contamination in resonators which may be tested empirically:

1. The change in surface contamination layers due to a change in temperature affects the mean resonant frequency of thickness-shear resonators. This frequency change may be masked by changes in material properties, such as elastic stiffnesses and density. Calculations for the 10 MHz resonator yield mean frequency changes of as much as 10 ppm.
2. The mean resonant frequency is also affected in the same order of magnitude by the ambient pressure which influences the characteristics of the surface contamination layers.
3. Magnitude of spectral density of frequency fluctuations for multilayer adsorption and desorption is larger than for monolayer adsorption and desorption. This is especially true when the value of E_v is close to E_l. Calculations for the 10 MHz resonator show that the magnitude of mean square frequency fluctuations is in the measurable range of about –120 dBc (Hz^2/Hz).
4. Spectral density of frequency fluctuations at 1 Hz for multilayer adsorption and desorption, when the value of E_v is close to E_l, is remarkably constant with changes in temperature. This is not so for monolayer adsorption and desorption.

Acknowledgement

The author gratefully acknowledge the support by the U.S. Army Research Office, contract no. DAAL03–87–K-0107. He thanks John R. Vig at the U.S. Army ETDL for his encouragement and support.

References.

1. Lu, C., and Czanderna, A.W., /Editors, Applications of Piezoelectric Quartz Crystal Microbalances, Methods and Phenomena, Their Applications in Science and Technology, Vol. 7, Elsevier (Amsterdam), 1984.
2. Yong, Y-K, and Vig, J.R., "Resonator Surface Contamination – A Cause of Frequency Fluctuations?" IEEE Transactions on Ultrasonics, Ferroelectrics, and Frequency Control, Vol. 36, No. 4, 1989, pp452–458.
3. Brunauer, S., Emmett, P.H., and Teller, E., Journal of the American Chemical Society, Vol. 60, 1938, pp309.
4. Adamson, A.W., Physical Chemistry of Surfaces, 4th edition, John Wiley, New York, 1982, pp533–539.
5. Ross, S.M., Introduction to Probability Models, 3rd edition, Academic Press, Orlando, 1985, chapt. 6 pp233–246.
6. Potter, M.C., and Goldberg, J., Mathematical Methods, 2nd edition, Prentice-Hall, Englewood Cliffs, 1987, pp293–295.
7. McWhorter, A.L., "1/f Noise and Germanium Surface Properties," Semiconductor Surface Physics, edited by R.H. Kingston, 1957, pp207–228.
8. Keshner, M.S., "1/f Noise," Proceedings of the IEEE, Vol. 70, No. 3, March 1982, pp212–218.

Fig.1 Adsorption of gases and vapors on solid surface[4], the BET model[3].

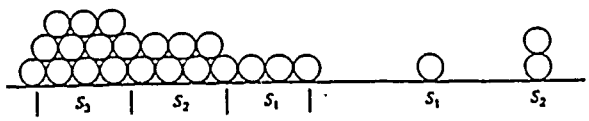

FIG.2 f–T curves for a 10 MHz thickness–shear resonator due to surface contamination. (Reference temperature=25 deg C, pressure=.001 torr, Ev=.75 E1)

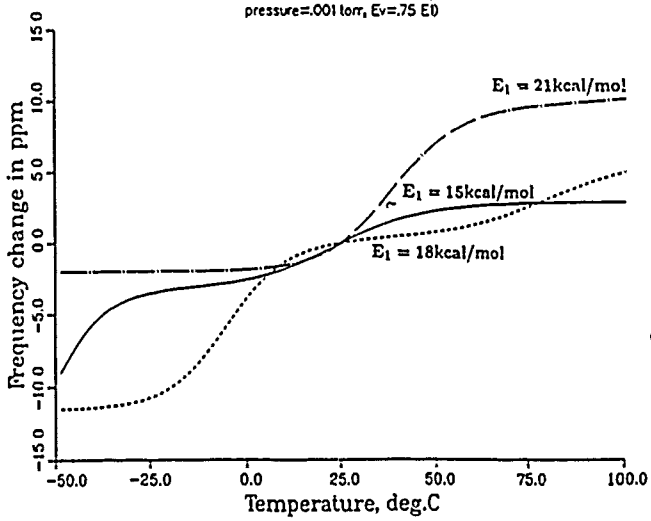

FIG.3 f–P curves for a 10 MHz thickness–shear resonator due to surface contamination. (Reference pressure=.001 torr, Ev=.75 E1 temperature=25 deg.C)

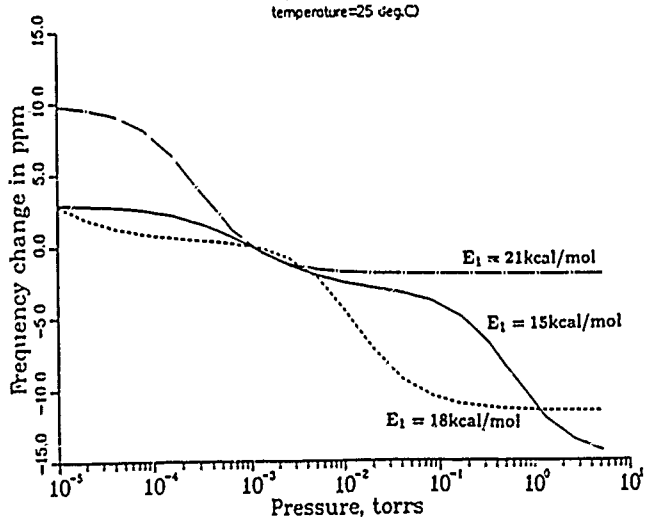

FIG.4 Spectral density of freq. fluctuations vs Fourier frequency. Pressure=1E–3 torr Temperature = 25 deg C. E1 = 21 kcal/mol

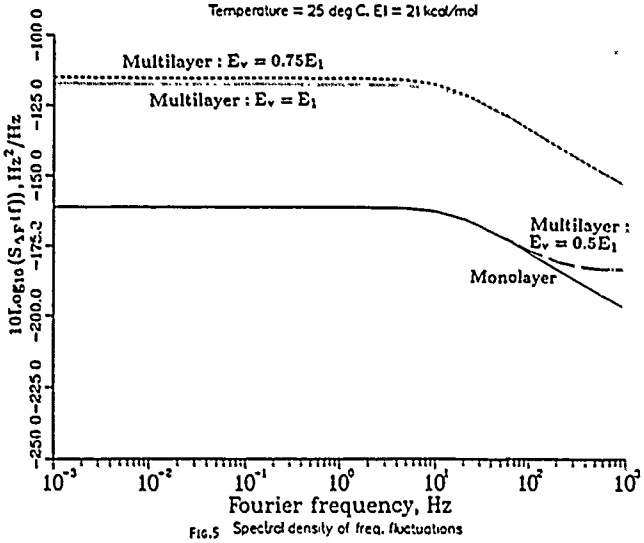

FIG.5 Spectral density of freq. fluctuations at 1 Hz vs pressure. Temperature = 25 deg C. E1 = 21 kcal/mol

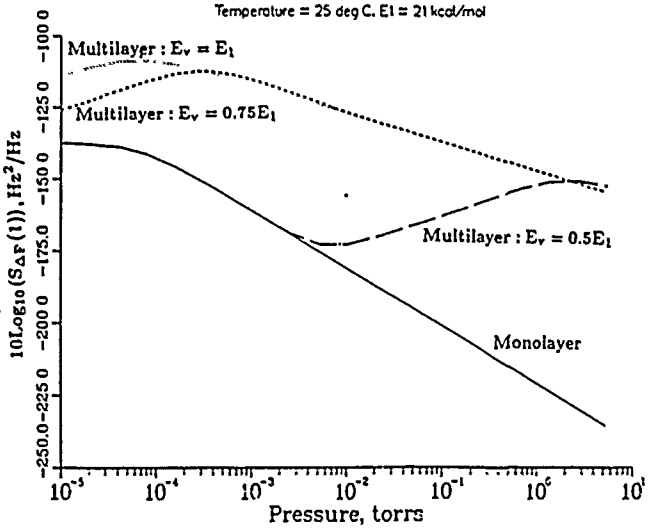

FIG.6 Spectral density of freq. fluctuations at 1 Hz vs temperature. Pressure = 1E–3 torr. E1 = 21 kcal/mol